

# Detectors in Nuclear and Particle Physics

Prof. Dr. Johanna Stachel

Department of Physics und Astronomy  
University of Heidelberg

May 13, 2015

## 3. Gas Detectors

### 3 Gas Detectors

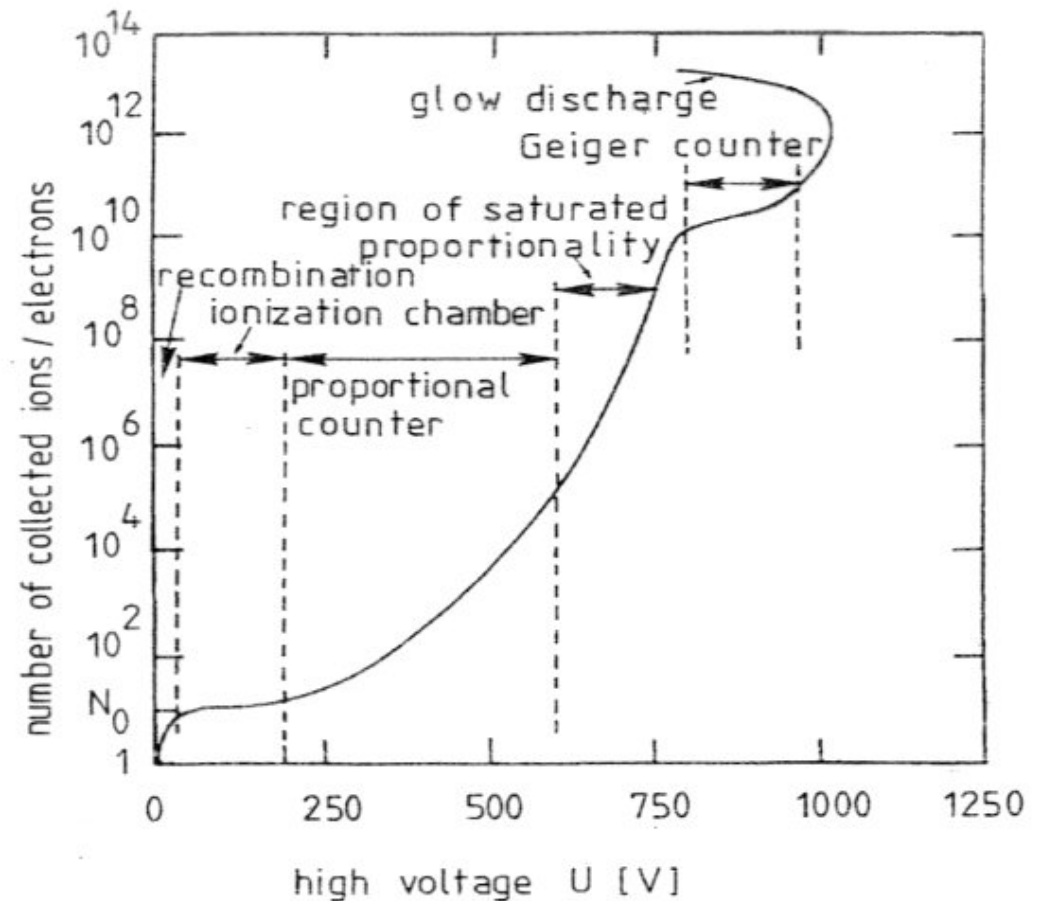
- General introduction
- Charge Transport
- Gas amplification
- Ionization chamber
- Proportional counter
- Drift chambers
- Cylindrical wire chambers
- Jet drift chambers
- Time Projection Chamber TPC

## 3.1 General introduction

### Principle

- ionizing particle creates primary and secondary charges via energy loss by ionization (Bethe-Bloch, chapter 2)  
 $N_0$  electrons and ions
- charges drift in electric field
- generally gas amplification in the vicinity of an anode wire
- signal generation

different operation modes depending on electric field strength



modes of operation of gas detectors (after F. Sauli 1977, lecture notes)

Charge carriers in layer of thickness  $L$  for a mean energy  $W$  to produce electron-ion pair

- mean number:

$$\langle n_t \rangle = \frac{L \langle \frac{dE}{dx} \rangle_{\text{ion}}}{W}$$

about 2 – 6 times the primary number (see chapter 2)

important for spatial resolution: **secondary ionization** by  $\delta$ -electrons happens on length scale  $10 \mu\text{m}$

e.g.  $T_e = 1 \text{ keV}$  in iso-butane  $\rightarrow R = 20 \mu\text{m}$

- ionization statistics:

$\lambda = 1/\sigma_I \rho$  mean distance between ionization events with cross section  $\sigma_I$

mean number of ionization events  $\langle n \rangle = L/\lambda$

Poisson distribution about mean  $\langle n \rangle$

$$P(n, \langle n \rangle) = \frac{\langle n \rangle^n \exp(-\langle n \rangle)}{n!}$$

and specifically probability for **no** ionization

$$P(0, \langle n \rangle) = \exp(-\langle n \rangle) = \exp(-L/\lambda)$$

**efficiency** of gas detectors allows determination of  $\lambda$  and hence  $\sigma_I$   
typical values:

	$\lambda \text{ (cm)}$
He	0.25
air	0.053
Xe	0.023

$$\rightarrow \sigma_I = 10^{-22} \text{ cm}^2 \text{ or } 100 \text{ b}$$

## 3.2 Charge Transport

### - Ion mobility

Ions drift along field lines in external E-field plus superimposed random thermal motion  
 ion transfers in collisions with gas atoms typically half of its energy  $\rightarrow$  kinetic energy of ion is approximately thermal energy

$$\langle T_{\text{ion}}(\vec{E}) \rangle \simeq \langle T_{\text{ion}}(\text{therm}) \rangle = \frac{3}{2} kT$$

drift velocity in direction of  $\vec{E}$ : develops from one collision to the next (thermal velocity has random orientation relative to  $\vec{E}$ )

assume instantaneous ion velocity due to electric field  $u_e = 0$  at  $t = 0$  and typical collision time  $\tau$

$\rightarrow$  directly prior to collision  $\vec{u}_e = \vec{a} \cdot \tau = \frac{e\vec{E}}{M} \cdot \tau$

$\rightarrow$  drift velocity of ion  $\vec{v}_{D+} = \langle \vec{u}_e \rangle = \frac{1}{2} u_e = \frac{e\vec{E}}{2M} \tau = \mu_+ \vec{E}$

$\mu_+ \equiv$  ion mobility

where  $\tau \propto \lambda \propto 1/\sigma_+ \simeq$  constant since  $\langle T_{\text{ion}} \rangle$  essentially thermal.

e.g.  $\text{C}_4\text{H}_{10}^+$  in  $\text{C}_4\text{H}_{10}$   $\mu_+ = 0.61 \frac{\text{cm/s}}{\text{V/cm}}$  at  $E = 1 \text{ kV/cm} \rightarrow v_{0+} = 0.6 \text{ cm/ms}$

typical drift distances **cm**  $\rightarrow$  typical ion drift times **ms**

# Electron mobility I

Electrons drift towards anode of a gas detector in a given field with a constant velocity, measurement of drift time allows to determine point of ionization.

$$\Delta t = \frac{L}{v_D}$$

equation of motion of electron in superimposed  $\vec{E}$  and  $\vec{B}$ -fields (Langevin):

$$m \frac{d\vec{v}}{dt} = e\vec{E} + e(\vec{v} \times \vec{B}) + \vec{Q}(t)$$

with instantaneous velocity  $\vec{v}$  and a stochastic, time dependent term  $Q(t)$  due to collisions with gas atoms

assume: collision time  $\tau$

$\vec{E}$  and  $\vec{B}$  constant between collisions

consider  $\Delta t \gg \tau$  (averaging)  $\rightarrow Q(t)$  is friction

steady state is reached when net force is zero, defines drift velocity  $v_D$

$$\langle m \frac{d\vec{v}}{dt} \rangle = e(\vec{E} + \vec{v}_D \times \vec{B}) - \underbrace{\frac{m}{\tau} \vec{v}_D}_{\text{Stokes-type}} = 0$$

## Electron mobility II

$$B = 0: \quad \vec{v}_D = \mu_- \vec{E} \quad \text{with} \quad \mu_- = \frac{e\tau}{m} \equiv \mu$$

$$B \neq 0: \quad \vec{v}_D = \mu_- \vec{E} + \omega\tau(\vec{v}_D \times \vec{B}) \quad \text{with Larmor frequency} \quad \omega = \frac{eB}{m} \quad (\text{see below})$$

Compared to ions,  $\mu_+ \ll \mu_-$  since  $M \gg m$

### 2 types of gases

- a) **hot gases:** atoms with few low-lying levels, electron loses little energy in a collision with atom  $\rightarrow T_e \gg kT$

acceleration in E-field and friction lead to constant  $v_D$  for a given  $\vec{E}$   
 'free fall with friction'

but  $\lambda(T_e) \simeq \lambda(|\vec{E}|)$  and  
 $\mu \propto \tau \propto 1/\sigma(|\vec{E}|)$  not constant.

typical drift velocity:  $v_D = 3 - 5 \text{ cm}/\mu\text{s}$  for 90% Ar/10% CH<sub>4</sub> (typically saturating with E)

- b) **cold gases:** many low-lying degrees of freedom  
 $\rightarrow$  electrons lose kinetic energy they gain in between collisions (similar to ions)

$$T_e \simeq kT \quad \mu \simeq \text{constant} \quad v_D \propto |E|$$

examples: Ar/CO<sub>2</sub> or Ne/CO<sub>2</sub>

in latter:  $\mu \simeq 7.0 \cdot 10^{-3} \text{ cm}^2/\mu\text{sV}$  at 10% CO<sub>2</sub>    or  $v_D = 2 \text{ cm}/\mu\text{s}$  at 300 V/cm  
 $3.5 \cdot 10^{-3} \text{ cm}^2/\mu\text{sV}$  at 20%     $v_D = 1 \text{ cm}/\mu\text{s}$

# Electron mobility III

Drift in combined  $\vec{E}$  and  $\vec{B}$ -fields

$$\vec{v}_D = \frac{\mu |\vec{E}|}{1 + \omega^2 \tau^2} \left[ \hat{E} + \underbrace{\omega \tau \hat{E} \times \hat{B}}_{\substack{\text{component} \\ \text{in direction} \\ \vec{E} \times \vec{B} \\ \propto \omega \tau}} + \underbrace{\omega^2 \tau^2 (\hat{E} \cdot \hat{B}) \hat{B}}_{\substack{\text{component} \\ \text{in direction} \\ \vec{B} \\ \propto (\omega \tau)^2}} \right]$$

$\hat{E}$ ,  $\hat{B}$ : unit vectors in direction of E- and B-field



# Electron loss

with some probability a free electron is lost during drift

a) recombination  $\text{ion}^+ + e^-$

decrease in number of negative (and positive) charge carriers

$$-\frac{dN^-}{dt} = p_r \cdot \rho^+ \rho^- \quad p_r : \text{coefficient of recombination} \simeq 10^{-7} \text{ cm}^3/\text{s}$$

generally not important

b) electron attachment

on electro-negative molecules, probability can be large



otherwise dissociative attachment



for gases like  $\text{O}_2$ ,  $\text{Cl}_2$ , freon,  $\text{SF}_6$  probability per collision is of order  $10^{-4}$

capture coefficient  $p_c$  is strongly energy dependent (in many gases there is a minimum at 1 eV 'Ramsauer effect')

electron undergoes order of  $10^{11}$  collisions/s  $\rightarrow$  for drift time of  $10^{-6}$  s fraction lost  $X_{\text{loss}}$  depends on partial oxygen pressure

$$X_{\text{loss}} = 10^{-4} \cdot (10^{11}/\text{s}) \cdot (10^{-6} \text{ s}) \cdot P_{\text{O}_2}/P_{\text{atm}}$$

$\rightarrow$  less than 1% lost for  $P_{\text{O}_2}/P_{\text{atm}} \leq 10^{-3}$

*Remark:* in presence of certain quencher gases such as  $\text{CO}_2$  the effect of  $\text{O}_2$  is enhanced by multistep catalytic reaction

- 10 ppm  $\text{O}_2$  can lead to 10% loss within  $10 \mu\text{s} \rightarrow$  need to keep oxygen level low in gas.

# Diffusion I

Original ionization trail diffuses (spreads apart) with drift time  
 → effect on space point and momentum resolution, ultimate limit

a) only thermal motion ( $|\vec{E}| = |\vec{B}| = 0$ )

mean thermal velocity

$$\langle v \rangle = \frac{\lambda}{\tau}$$

$\lambda$  mean free path

$\tau$  time between collisions

$$\langle T_e \rangle = \frac{1}{2} m \langle v \rangle^2$$

for a point-like source at time  $t = 0$ , collisions between electrons and gas atoms (molecules)  
 → smearing: spread of charge cloud at time of first collision

$$R^2 = 2\lambda^2$$

and after  $n = t/\tau$  collisions

$$\sigma^2(t) = 2\lambda^2 t/\tau$$

define **diffusion coefficient**

$$D = \frac{\sigma^2(t)}{2t}$$

$$\text{for } |\vec{E}| = |\vec{B}| = 0 \quad D = D_0 = \frac{\lambda_0^2}{\tau} = \frac{2\langle T_e \rangle}{m} \tau$$

# Diffusion II

diffusion is **isotropic**

longitudinal diffusion coefficient  $D_{0L} = \frac{1}{3} \frac{\lambda_0^2}{\tau}$

transverse diffusion coefficient  $D_{0T} = \frac{2}{3} \frac{\lambda_0^2}{\tau}$

→ after time  $t$  charge cloud has width  $\sigma(t) = \sqrt{D2t}$

respectively, in each dimension  $\sigma_x(t) = \sigma_y(t) = \sigma_z(t) = \sqrt{\frac{1}{3} D2t}$

charge distribution Gaussian  $N(x) = c \cdot \exp\left(-\frac{x^2}{2\sigma_x^2}\right)$

diffusion equation: charge density  $\rho(\vec{r}, t)$  for conserved electron current  $\vec{j}$  defined by

$$\frac{\partial \rho}{\partial t} + \nabla \cdot \vec{j} = 0$$

without field,  $\vec{j} = -D\nabla\rho \Rightarrow \frac{\partial \rho}{\partial t} = D\Delta\rho$

solved by  $\rho(\vec{r}, t) = c \cdot \exp\left(-\frac{\vec{r}^2}{4Dt}\right)$

# Diffusion III

hot gases:  $\langle T_e \rangle \gg \frac{3}{2} kT$   $D$  large

cold gases:  $\langle T_e \rangle \simeq \frac{3}{2} kT$   $D$  small

with 1-dim diffusion  $D = \frac{2\langle T_e \rangle}{3m} \tau$

and  $\mu = \frac{e}{m} \tau$  (B=0)

$$\langle T_e \rangle = \frac{3}{2} e \frac{D}{\mu}$$

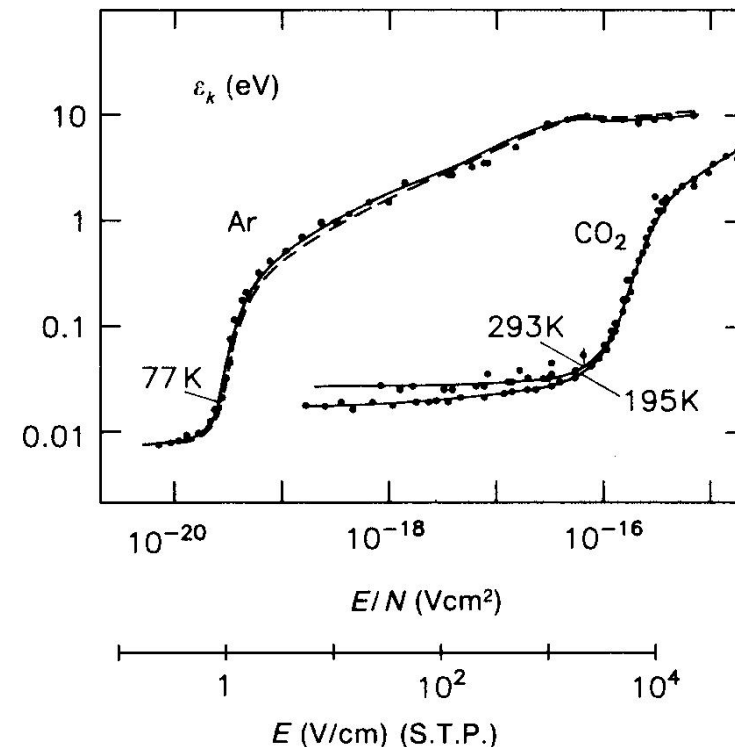
can define a characteristic energy

$$\epsilon_k = \frac{2}{3} \langle T_e \rangle = e \frac{D}{\mu}$$

diffusion of cloud after distance  $L$

$$\sigma_x^2 = 2Dt = 2D \frac{L}{\mu E} = \frac{2\epsilon_k}{eE} L \quad (1)$$

for hot gas the same characteristic energy is reached at much lower  $T$



characteristic energy of electrons in Ar and CO<sub>2</sub> as a function of the reduced  $E$ . The electric field under normal conditions is also indicated. The parameters refer to temperatures at which the measurements were made.

# Diffusion IV

## b) diffusion in B-field

$$\vec{B} = B\vec{e}_z$$

along  $B$  no Lorentz force

$$D_L(B) = D_{0L} = \frac{1}{3} D_0$$

in transverse direction Lorentz force  
helps to keep charge cloud together, i.e.  
it counteracts diffusion

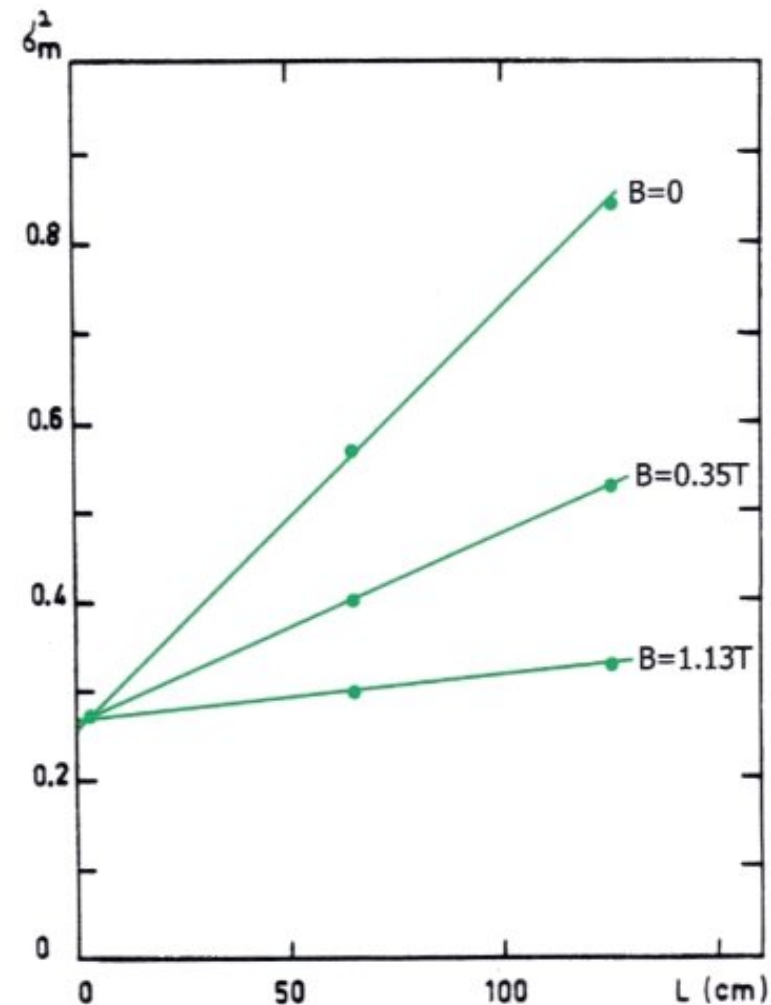
$$D_T(B) = \frac{D_{0T}}{1 + \omega^2 \tau^2}$$

for  $\vec{B}$  large

$$\rightarrow \omega\tau \gg 1 \quad D_T(B) \ll D_{0T}$$

e.g. Ar/CH<sub>4</sub> at

$$B = 1.5 \text{ T} \quad D_T(1.5 \text{ T}) \simeq \frac{1}{50} D_{0T}$$



transverse  $\sigma^2$  as function of  $L$

# Diffusion V

c) diffusion in electric field:  
 ordered drift along field superimposed to  
 statistical diffusion  
 mobility  $\mu$  is function of  $\langle T_e \rangle$

$$\vec{v}_D = \mu(\langle T_e \rangle) \cdot \vec{E}$$

→ energy spread leads to longitudinal  
 spreading of electron cloud  $D_L \neq \frac{1}{2} D_T$

statistical transverse diffusion not affected  
 by E-field

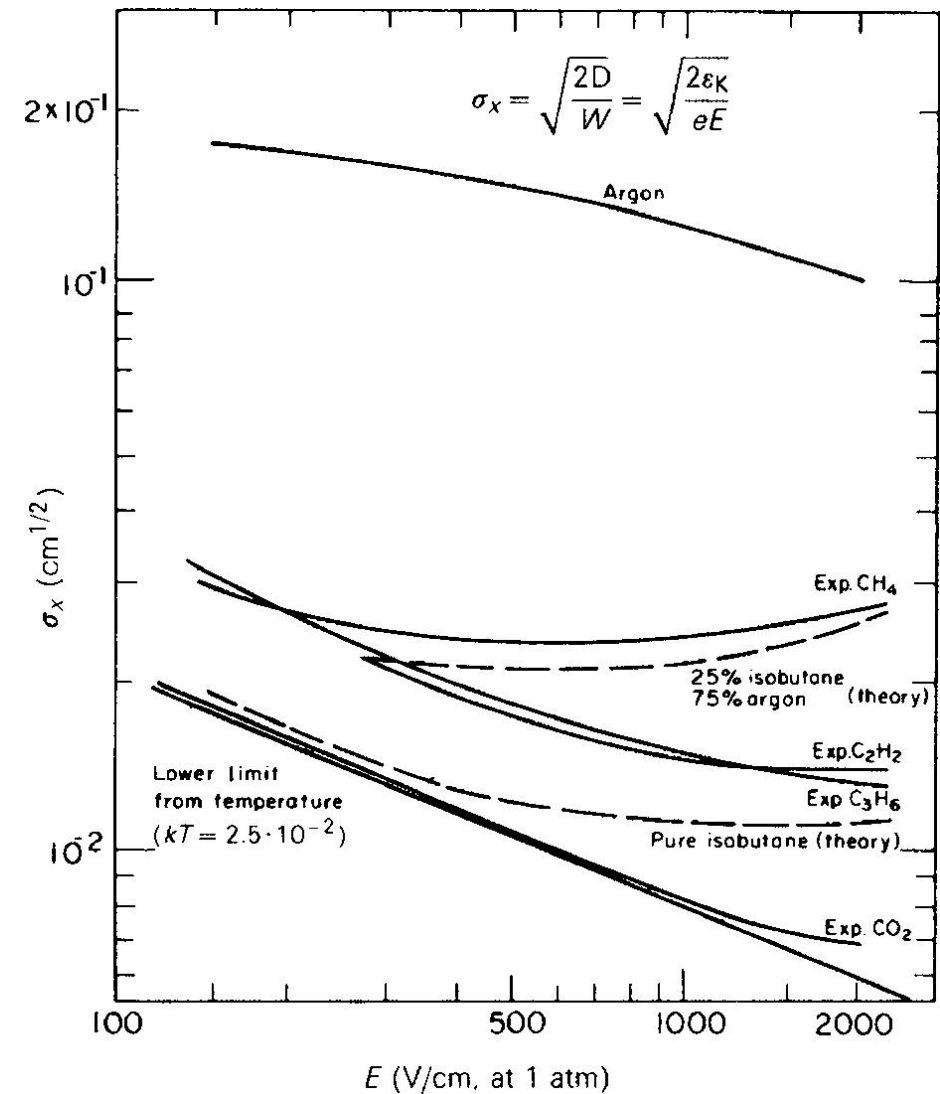
in hot gases:

for large  $E$ ,  $D_L > D_T$  and values are large

in cold gases:  $D_L \simeq D_T$  small

$$\sigma^2(t) = 2Dt = 2D \frac{L_D}{v_D} = \frac{2kT}{e|\vec{E}|} L_D$$

$$\frac{\sigma^2(t)}{L_D} = \frac{2kT}{e|\vec{E}|}$$



longitudinal diffusion width  $\sigma_x / \sqrt{L_D}$  after 1 cm of drift

# Exact solution

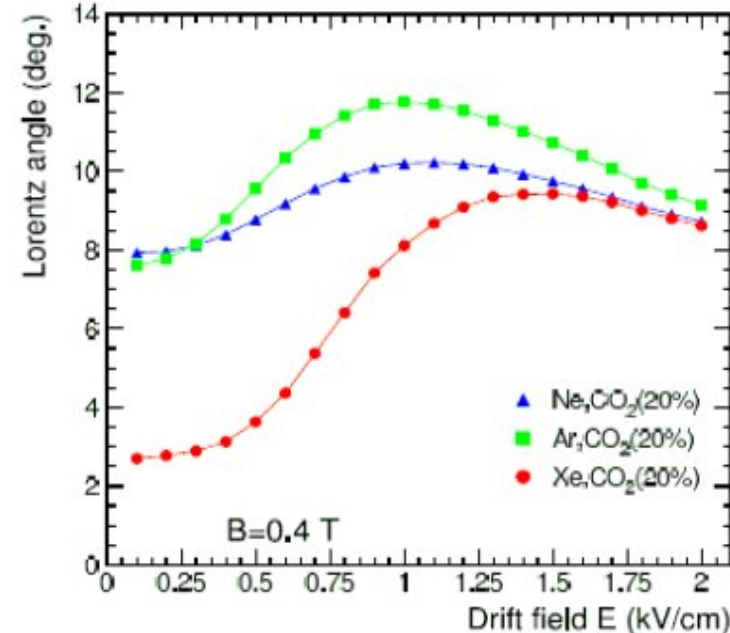
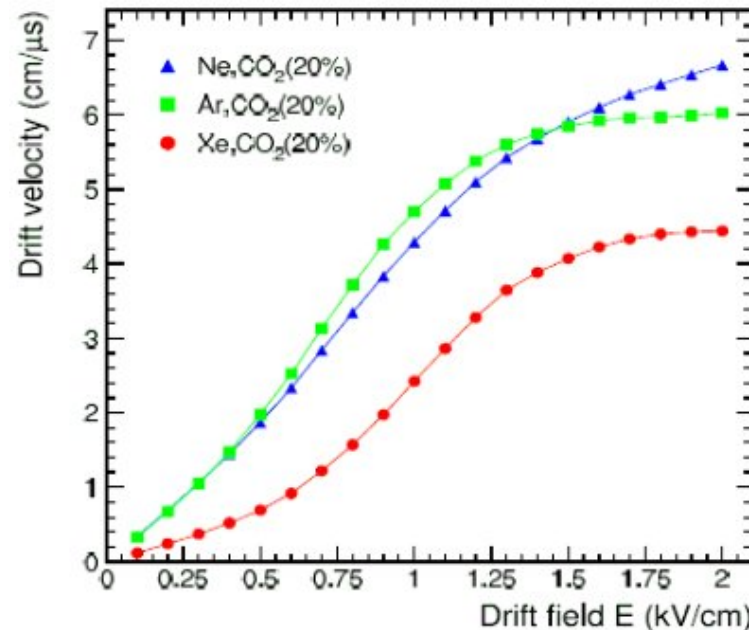
of drift and diffusion by solving a 'transport equation' for electron density distribution  $f(t, \vec{r}, \vec{v})$

Boltzmann-equation:

$$\frac{\partial f}{\partial t} + \underbrace{\vec{v} \frac{\partial}{\partial \vec{r}} f}_{\text{flow term}} + \underbrace{\frac{\partial}{\partial \vec{v}} \vec{g}}_{\text{external forces}} = \underbrace{Q(t)}_{\text{collision term (stochastic)}}$$

$$\vec{g} = \left( \frac{e\vec{E}}{m} + \vec{\omega} \times \vec{v} \right) f$$

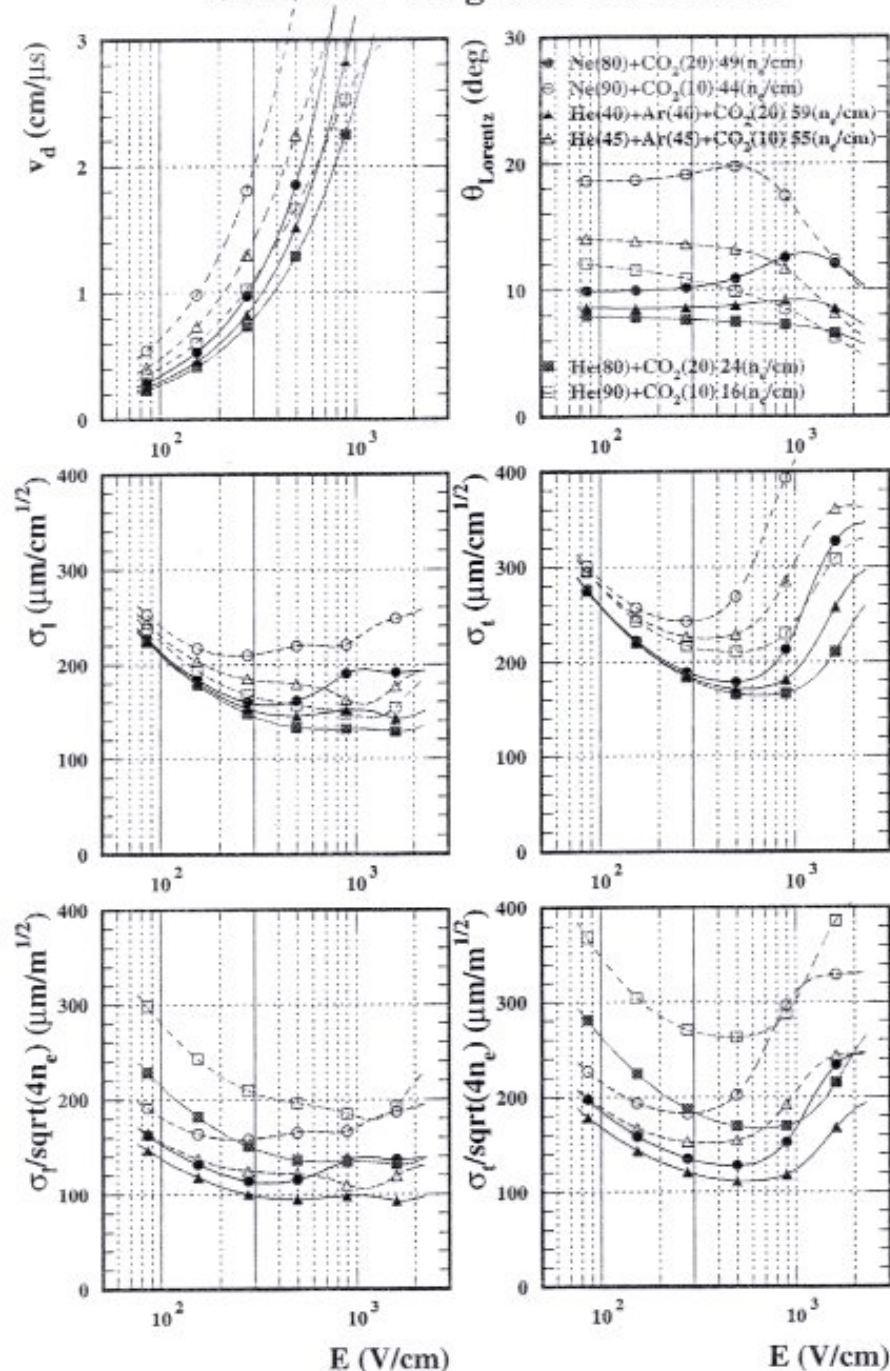
numerical solution with codes such as Magboltz & Garfield



Lorentz angle: angle between E-field and drift velocity of electrons in presence of B not  $\perp$  to E



## Garfield + Magboltz calculation



Drift velocity (top left), Lorentz angle (top right), longitudinal and transverse diffusion constants (middle) and longitudinal and transverse diffusion constants normalized to the square root of the number of charge carriers (bottom) for different mixtures of noble gas and CO<sub>2</sub>.

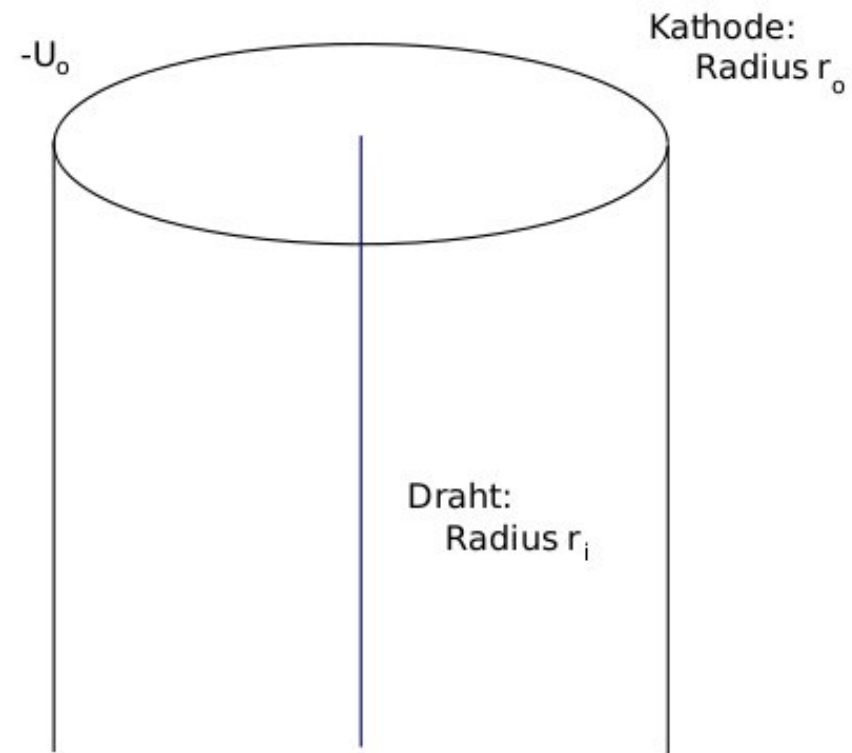
Lorentz angle: angle between E-field and drift velocity of electrons in presence of B not  $\perp$  to E



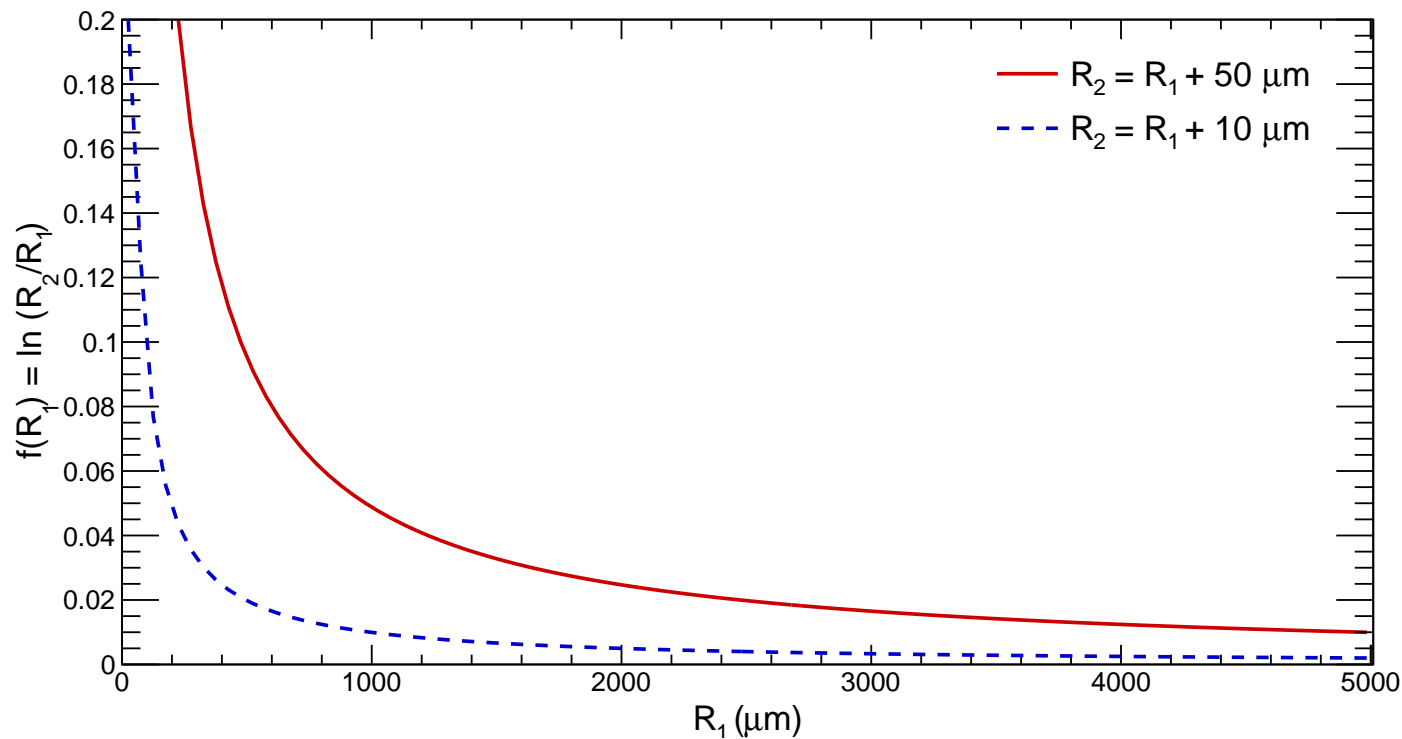
### 3.3 Gas amplification

in case the anode is a (thin) wire, E-field in vicinity of wire very large  $E \propto 1/r$   
and the electron gains large kinetic energy.

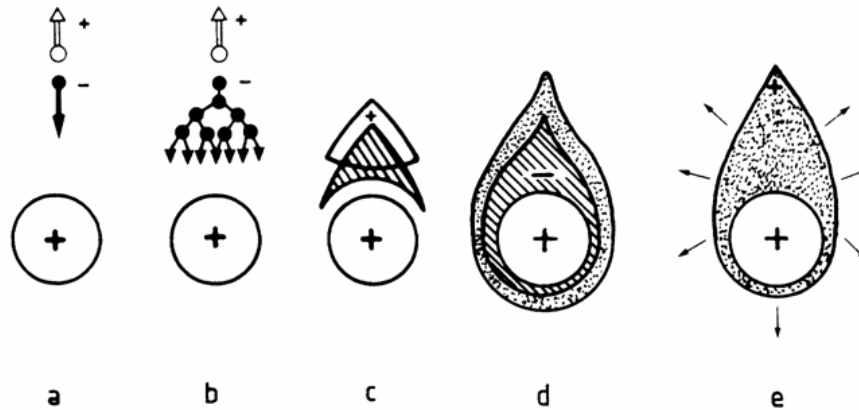
$$\begin{aligned}
 \Delta T_e &= e\Delta U \\
 &= e \int_{r_1}^{r_2} E(r) dr \\
 &= \frac{eU_o}{\ln r_o/r_i} \int_{r_1}^{r_2} \frac{1}{r} dr \\
 &= eU_o \frac{\ln r_2/r_1}{\ln r_o/r_i}
 \end{aligned}$$



in order to obtain large  $E$  and hence large  $\Delta T_e$  we use very thin wires ( $r_i \simeq 10 - 50 \mu m$ )  
within few wire radii  $\Delta T_e$  is large enough for secondary ionization  
strong increase of  $E \rightarrow$  avalanche formation for  $r \rightarrow r_i$ .



# Avalanche formation in vicinity of a thin wire



Temporal and spatial development of an electron avalanche

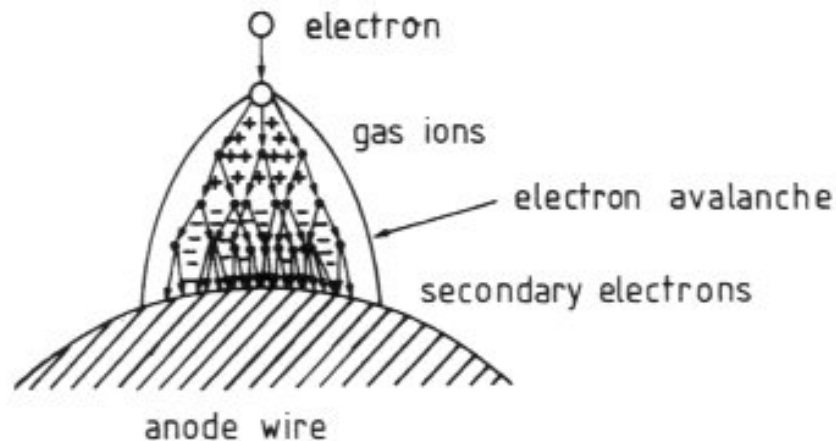
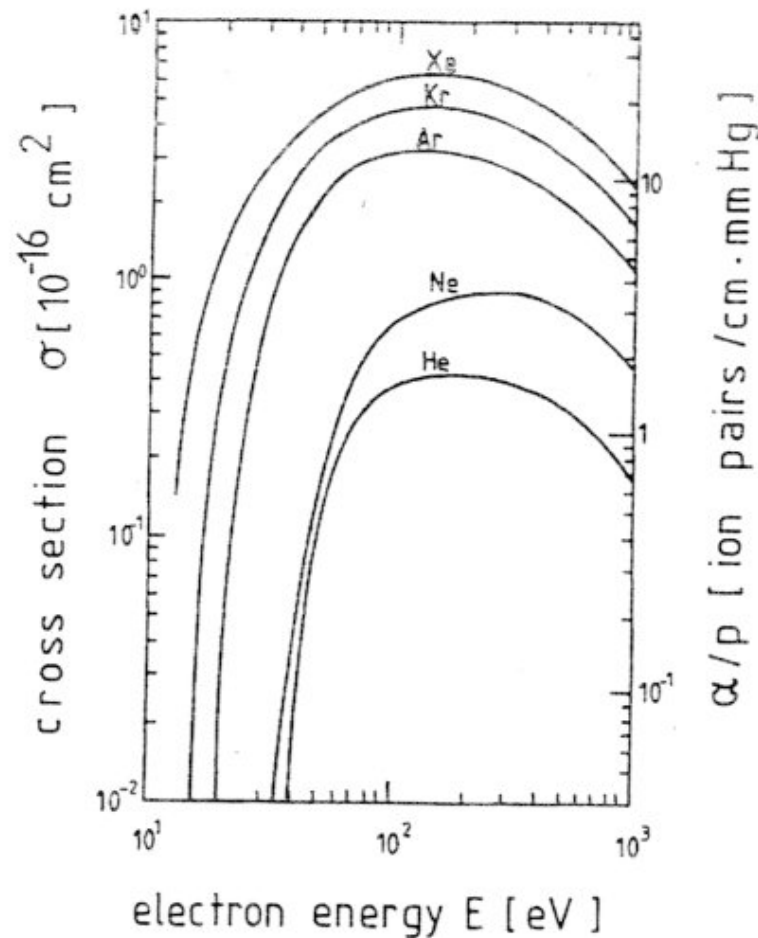


Illustration of the avalanche formation on an anode wire in a proportional counter. By lateral diffusion a drop-shaped avalanche develops.

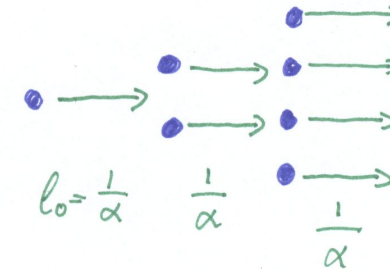


Photographic reproduction of an electron avalanche. The photo shows the form of the avalanche. It was made visible in a cloud chamber by droplets which have condensed on the positive ions.

# First Townsend coefficient $\alpha$



Energy dependence of the cross section for ionization by collision.



number of electrons  $N(x) = N_0 \underbrace{\exp \alpha x}_{\text{gas gain}}$

mean free path  $l_0 = 1/\alpha = 1/(N\sigma(T_e))$

$$T_e = T_e(E(x))$$

$$\Rightarrow \alpha = \alpha(x)$$

gas gain

$$G = \exp \left( \int_{r_1}^{r_2} \alpha(x) dx \right)$$

Typically  $10^4 - 10^5$ , up to  $10^6$  possible in proportional mode.

**limit:** discharge (spark) at  $\alpha x \simeq 20$

or  $G = 10^8$  'Raether-limit'

## Second Townsend coefficient

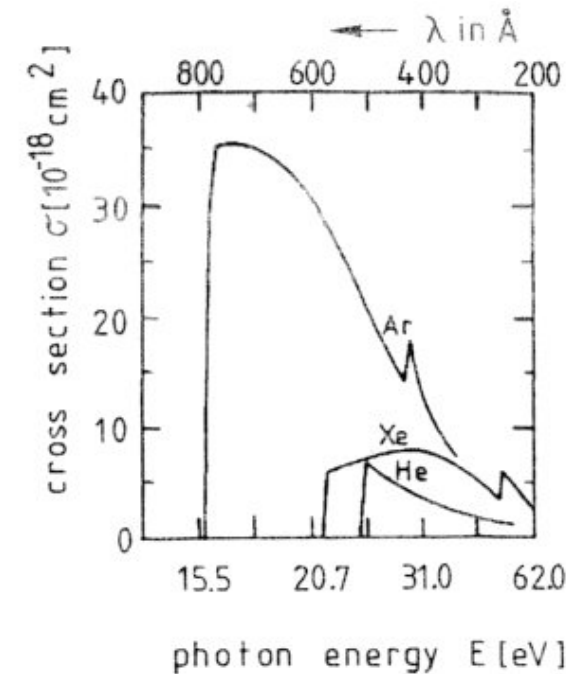
excitation of gas generates UV-photons which in turn can lead to photo effect in gas and on cathode wire contributing thus to avalanche.

$$\gamma = \frac{\# \text{ photo effect events}}{\# \text{ avalanche electrons}}$$

gas gain including photo effect

$$G_{\gamma} = \underbrace{G}_{\text{no}} + \underbrace{G(G\gamma)}_{\text{one}} + \underbrace{G(G\gamma)^2}_{\text{two}} + \dots = \frac{G}{1 - \gamma G}$$

photo effect events



Energy dependence of the cross section for photoionization

limit:  $\gamma G \rightarrow 1$  continuous discharge independent of primary ionization

to prevent this, add to gas so-called **quench-gas** which absorbs UV photons strongly, leading to excitation and radiationless transitions

examples:  $\text{CH}_4$ ,  $\text{C}_4\text{H}_{10}$ ,  $\text{CO}_2$

## 3.4 Ionization chamber

no gas gain, charges move in electric field and induce signal in electrodes.

2 electrodes form parallel plate capacitor.

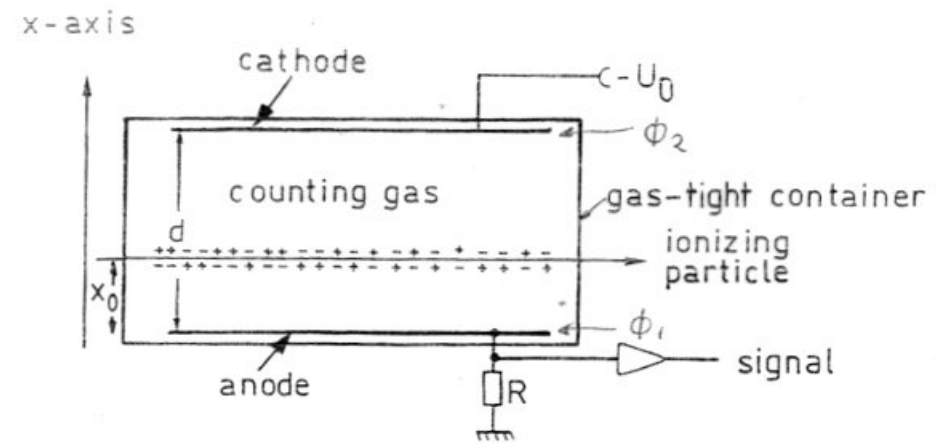
consider motion of a free charge  $q$ : electric field does work, capacitor is charged (lowering in energy of capacitor).

$$q \vec{\nabla} \Phi \cdot d\vec{x} = dq_i \cdot U_0$$

leads to induced current

$$I_{\text{ind}} = \frac{q}{U_0} \vec{\nabla} \Phi \cdot \vec{v}_D$$

$$\text{with } \vec{E} = -\vec{\nabla} \Phi \text{ and } U_0 = \Phi_1 - \Phi_2$$



Principle of operation of a planar ionization chamber

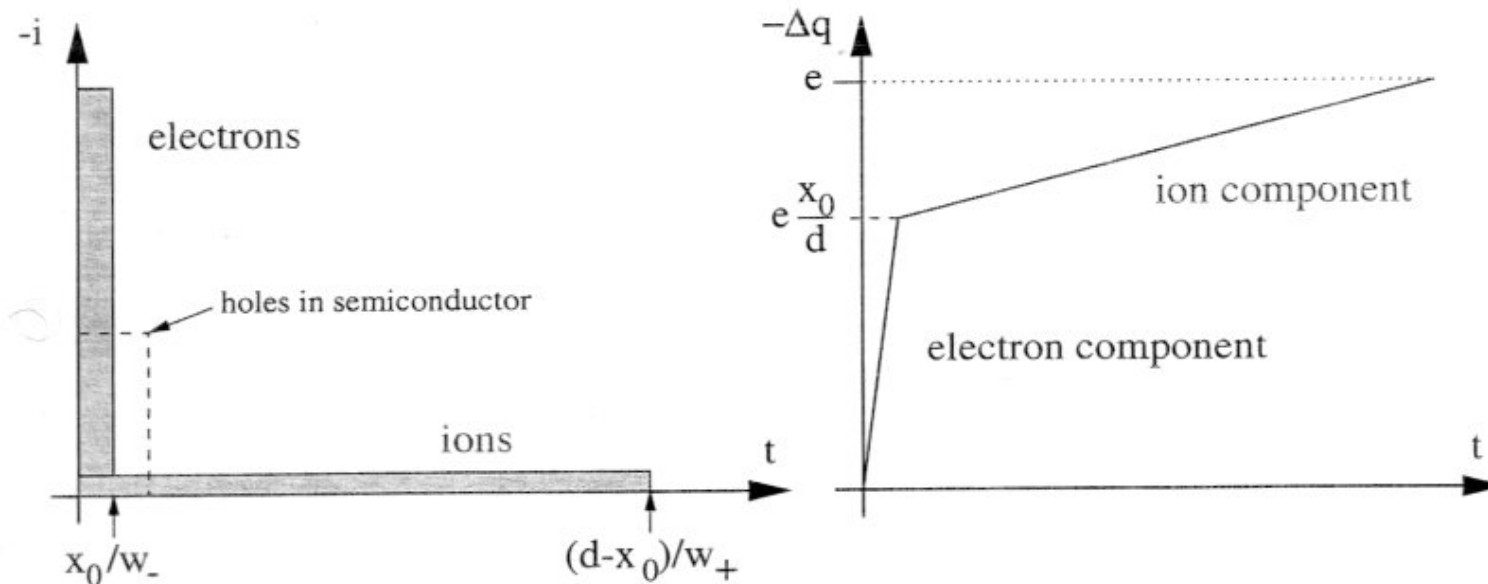
- current is constant **while** charge is drifting
- total induced signal (charge) independent of  $x_0$

- signal induced by electrons 
$$\Delta q_- = \frac{N_e}{U_0} (\Phi(x_0) - \Phi_1)$$

- signal induced by ions 
$$\Delta q_+ = -\frac{N_e}{U_0} (\Phi(x_0) - \Phi_2)$$

- $|N_{ion}| = |N_e|$ , but opposite charge  $\rightarrow$  **total  $\Delta q = \Delta q_- + \Delta q_+ = N_e$**

practical problem: ion comparatively slow  $w_+ = 10^{-3} \dots 10^{-2} w_-$  (see mobilities above)  
(except for semiconductors: typ.  $w_+ \approx 0.5 w_-$ )



Induced current and charge for parallel plate case, ratio  $w_-/w_+$  decreased for purpose of illustration.

## signal generated during drift of charges

- induced current ends when charges reach electrodes
- induced charge becomes constant (total number  $N_e$ )
- signal shaping by differentiation (speed of read-out)  $\rightarrow$  suppresses slow ion component

change in potential  $dU = \frac{dQ}{C}$

$U_0$  = external voltage

typical time constant of power supply (+ cables ...)

$$RC \gg \Delta t^-, \Delta t^+$$

usually electronic signal shaping needed

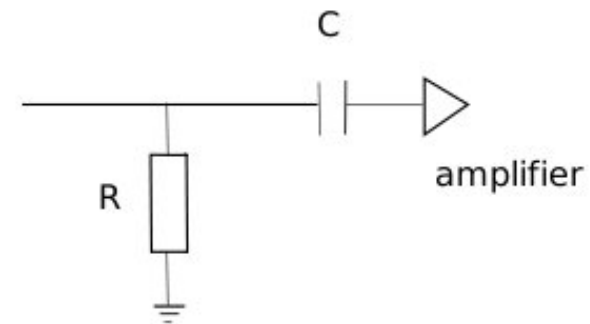
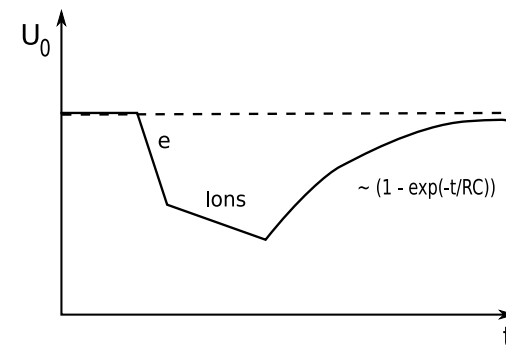
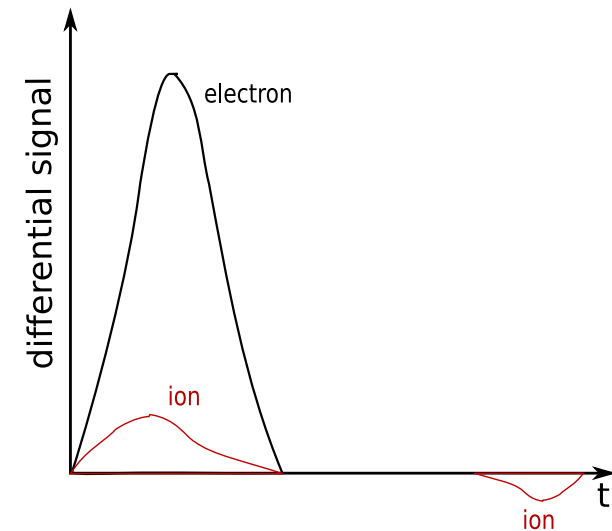
## Signal shaping by RC-filter

choose e.g.  $\Delta t^- \ll RC \ll \Delta t^+$

damps ion component

$$\begin{aligned} \Delta U &= \Delta U^- + \Delta U^+ \\ &= \frac{\Delta Q^-}{C} + \frac{\Delta Q^+}{C} \end{aligned}$$

where  $\Delta Q^{+-}$  is the charge induced in the anode by motion of ions and electrons for total number of ionization events in gas  $N_e$





$$\Delta Q^- = N_e \frac{\Phi(x_0) - \Phi_1}{U_0}$$

$$= N_e \frac{x_0}{d}$$

$$\Delta Q^+ = -N_e \frac{\Phi(x_0) - \Phi_2}{U_0}$$

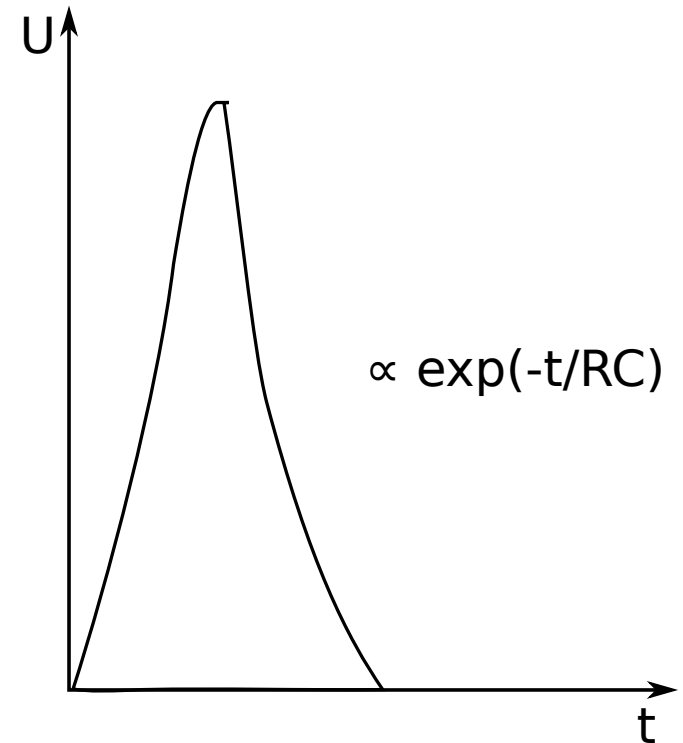
$$= N_e \frac{d - x_0}{d}$$

$$\text{without filter } \Delta Q = N_e, \quad \Delta U = \frac{N_e}{C}$$

$$\text{with filter } d - x_0 = v^+ \Delta t^+$$

$$\rightarrow v^+ RC \left( 1 - \exp\left(-\frac{\Delta t^+}{RC}\right) \right)$$

damping of ion component



fast rise and decrease of signal but now pulse height depends on  $x_0$

**trick:** introduce additional grid: “Frisch grid”  
 while electrons drift towards Frisch grid, no induced signal on anode, only on Frisch Grid  
 as soon as electrons pass Frisch grid, signal induced on anode  
 choose  $U_g$  such that the  $E$ -field is unchanged

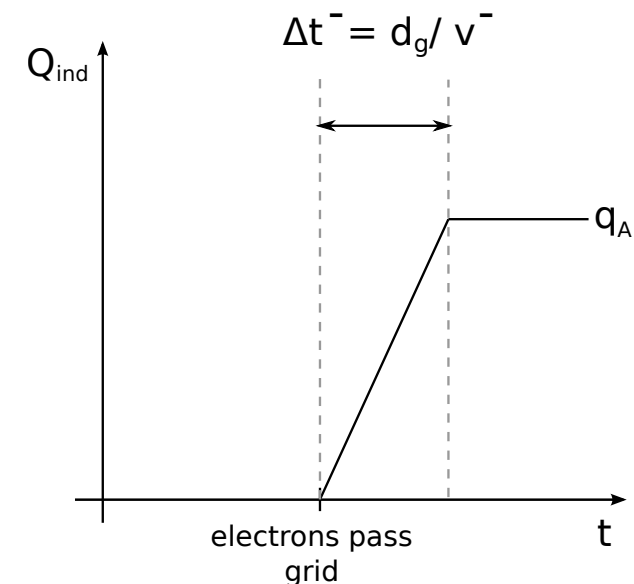
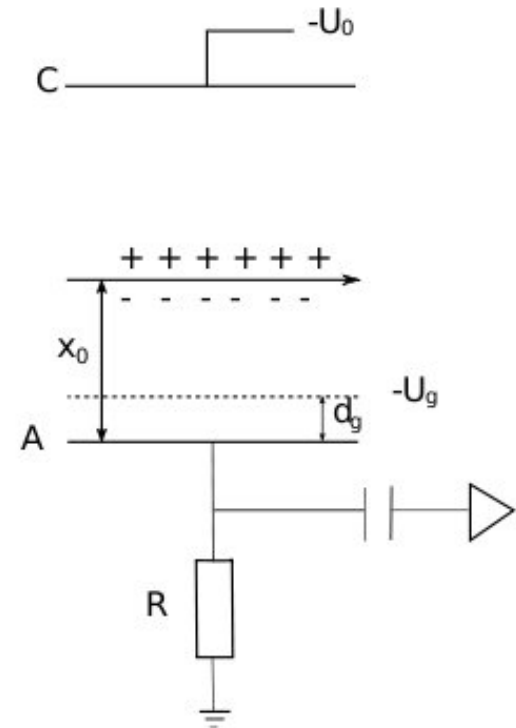
$$\Delta Q = \Delta Q^- = N_e$$

$$\Delta t^- = \frac{d_g}{v^-}$$

**general difficulty for ionization chambers:** small signals  
 example: 1 MeV particle stops in gas

$$\begin{aligned} N_e &\simeq \frac{10^6 \text{ eV}}{35 \text{ eV}} \simeq 3 \cdot 10^4 \\ C &\simeq 100 \text{ pF} \\ \Rightarrow \Delta U_{\max} &= \frac{3 \cdot 10^4 \cdot 1.6 \cdot 10^{-19} \text{ C}}{10^{-10} \text{ F}} \\ &= 4.6 \cdot 10^{-5} \text{ V} \end{aligned}$$

need sensitive, low-noise preamplifier

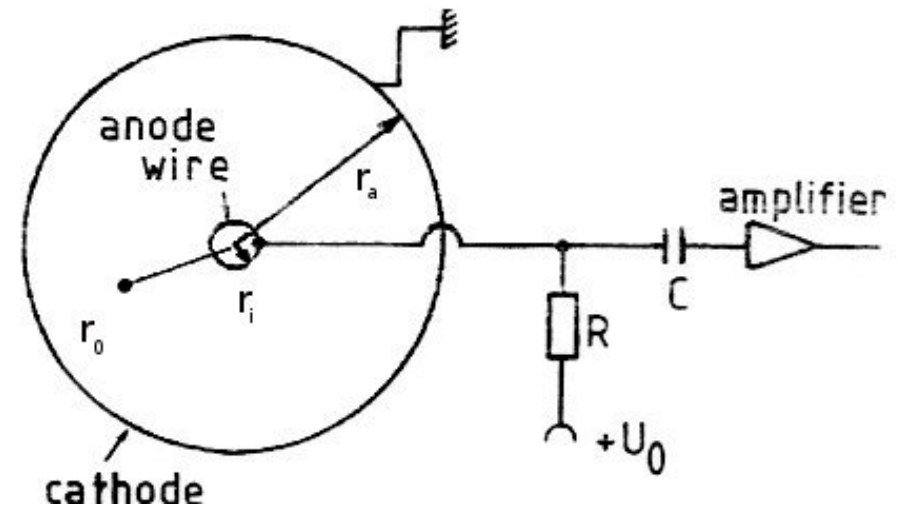


**application:** e.g. cylindrical ionization chamber for radiation dosimetry

$$\vec{E}(r) = -\frac{U_0}{r \ln r_a/r_i} \hat{e}_r$$

ionization at radius  $r_0$ :

$$\begin{aligned} \Delta t^- &= \int_{r_0}^{r_i} \frac{dr}{v^-(r)} = - \int \frac{dr}{\mu^- E} \\ &= - \int_{r_0}^{r_i} \frac{dr}{\mu^- U_0} r \ln \frac{r_a}{r_i} \\ &= \frac{\ln(r_a/r_i)}{2\mu^- U_0} (r_0^2 - r_i^2) \end{aligned}$$



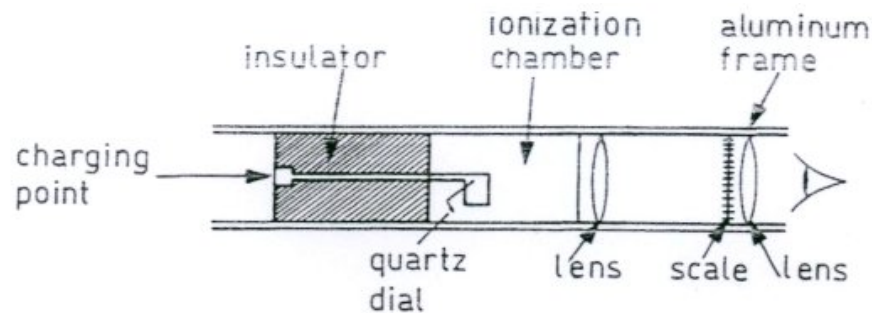
Principle of operation of a cylindrical ionization chamber

$l_0$ : typical ionization length, the centroid of the avalanche is this amount away from the wire

$$\begin{aligned} \Delta Q^- &= \frac{N_e}{U_0} \int E(r) dr = \frac{N_e}{\ln(r_a/r_i)} \ln \frac{r_i}{l_0} & \Delta U^- &= \Delta Q^- / C \\ \frac{\Delta U^+}{\Delta U^-} &= \frac{\ln(r_a/l_0)}{\ln(r_i/l_0)} & r_a \gg r_i &\rightarrow \Delta U^+ \gg \Delta U^- \end{aligned}$$

in cylindrical geometry, ion signal dominates by typically factor 100.

# Dosimeter for Ionization



Construction of an ionization pocket dosimeter

- cylindrical capacitor filled with air
- initially charged to potential  $U_0$
- ionization continuously discharges capacitor
- reduction of potential  $\Delta U$  is measure for integrated absorbed dose (view e.g. via electrometer)

**other applications:** measure energy deposit of charged particle, should be highly ionizing (low energy) or even stop (then measure total kinetic energy)  
 nuclear physics experiments with energies of 10 to 100 MeV  
 combination of  $\Delta E$  and  $E$  measurements  $\rightarrow$  particle identification (nuclei)

## 3.5 Proportional Counter

gas amplification as described above

$$N = A \cdot N_e$$

with a gas gain in vicinity of wire

$$A = \exp \int_{r_k}^{r_i} \alpha(x) dx$$

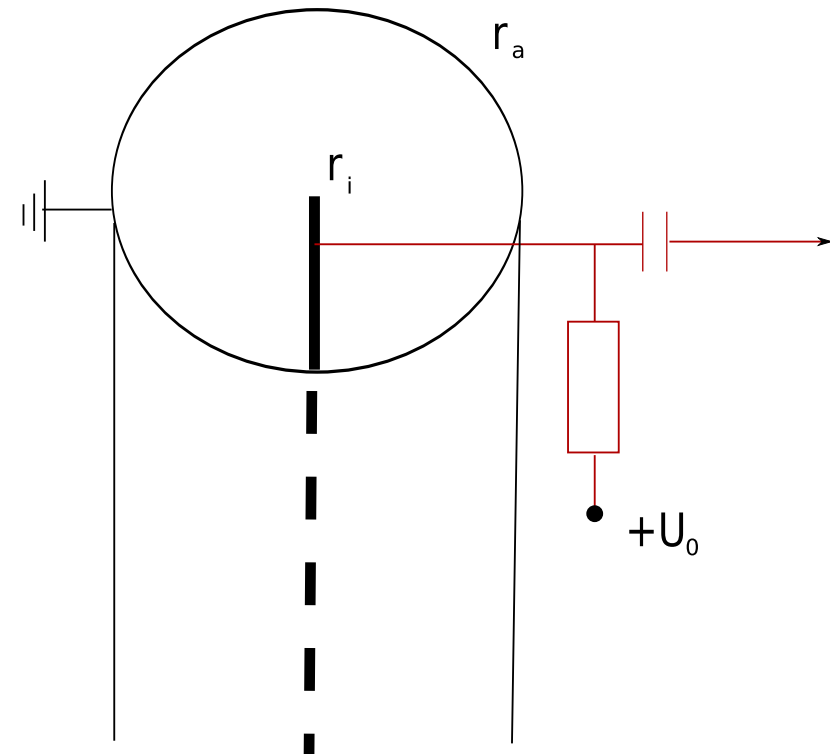
charge avalanche typically builds up within  $20 \mu m$

effectively it starts at  $r_0 = r_i + k\lambda$

$k$ : number of mean free paths needed for avalanche formation

$\lambda$ : mean free paths of electrons (order  $\mu m$ )

$$(2^{10} \cong 1000 \quad 2^{17} \cong 10^5)$$



$$\Delta U^- = - \frac{N_e A}{C} \frac{\ln r_0 / r_i}{\ln r_a / r_i}$$

$$\Delta U^+ = - \frac{N_e A}{C} \frac{\ln r_a / r_0}{\ln r_a / r_i}$$

$$\frac{\Delta U^+}{\Delta U^-} = \frac{\ln r_a/r_0}{\ln r_0/r_i} = R$$

$$r_a = 1 \text{ cm}, r_i = 30 \text{ } \mu\text{m}, k\lambda = 20 \text{ } \mu\text{m} \text{ for Ar at } P_{\text{atm}} \rightarrow R \simeq 10$$

**In a proportional counter the signal at the anode wire is mostly due to ion drift!**

rise time for electron signal as discussed above

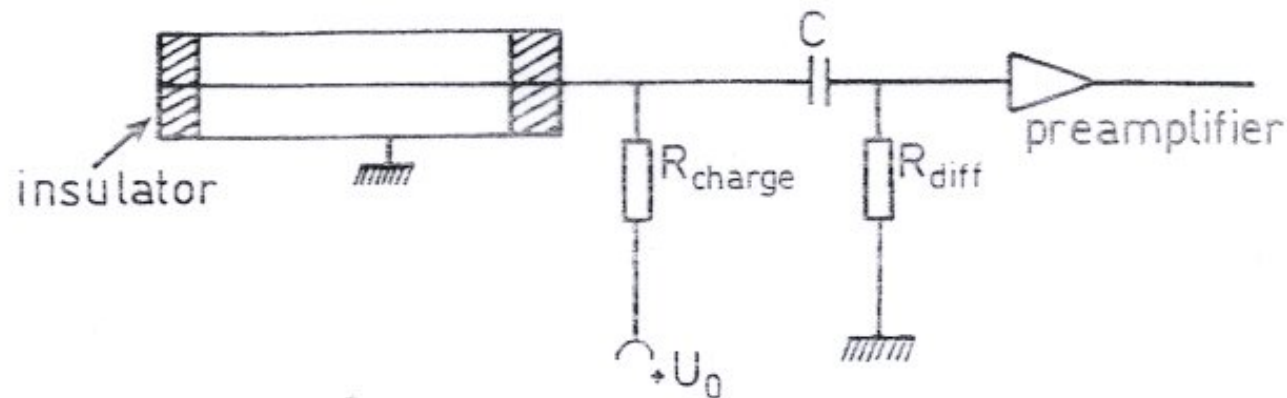
$$\Delta t^- = \frac{\ln(r_a/r_i)}{2\mu^- U_0} (r_0^2 - r_i^2) \quad \text{order of ns for } \mu^- = 100 - 1000 \text{ cm}^2/\text{Vs}$$

and  $U_0 \cong \text{several } 100 \text{ V}$

ion signal  $\Delta t^+$  slow, order of 10 ms  $\rightarrow$  differentiate with  $R_{\text{diff}} \cdot C$

**in case  $R_{\text{diff}} \cdot C = 1 \text{ ns} \rightarrow$  time structure of individual ionization clusters can be resolved**

## Typical set-up



Readout of a proportional counter

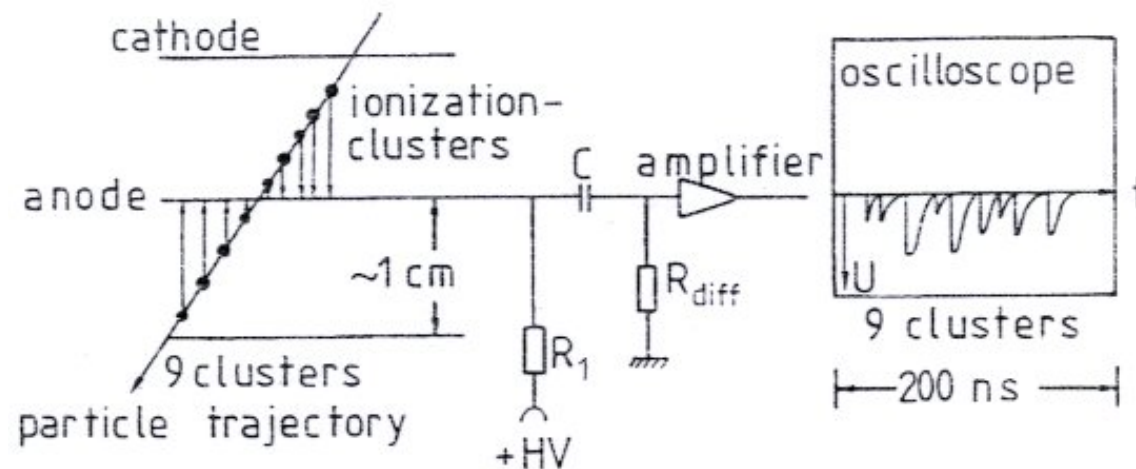


Illustration of the time structure of a signal in the proportional counter

**Application outside particle physics:** particularly suited to measure X-rays, e.g. 'X-ray imaging' with special electrode geometries for experiments involving synchrotron radiation (high rates!)

# Multi-wire proportional chamber

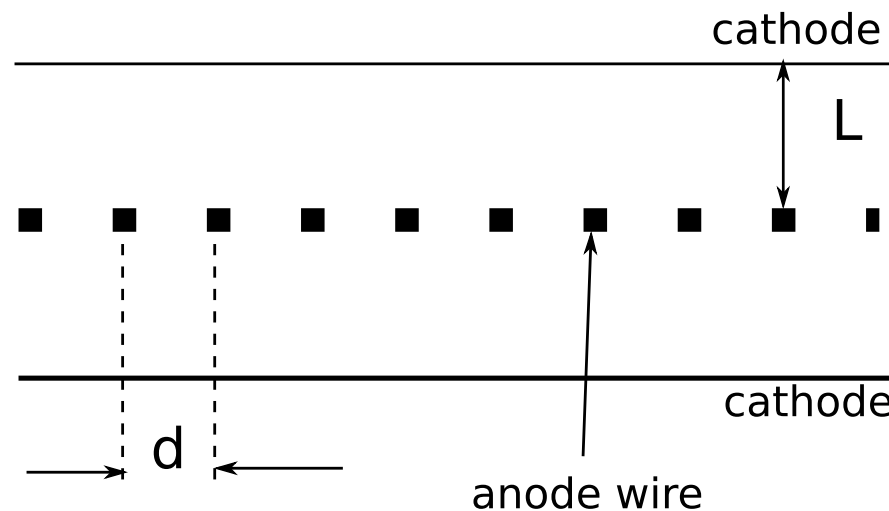
most important application:

## Multi-wire proportional chamber **MWPC**

planar arrangement of proportional counters without separating walls

G. Charpak et al. NIM 62 (1968) 202

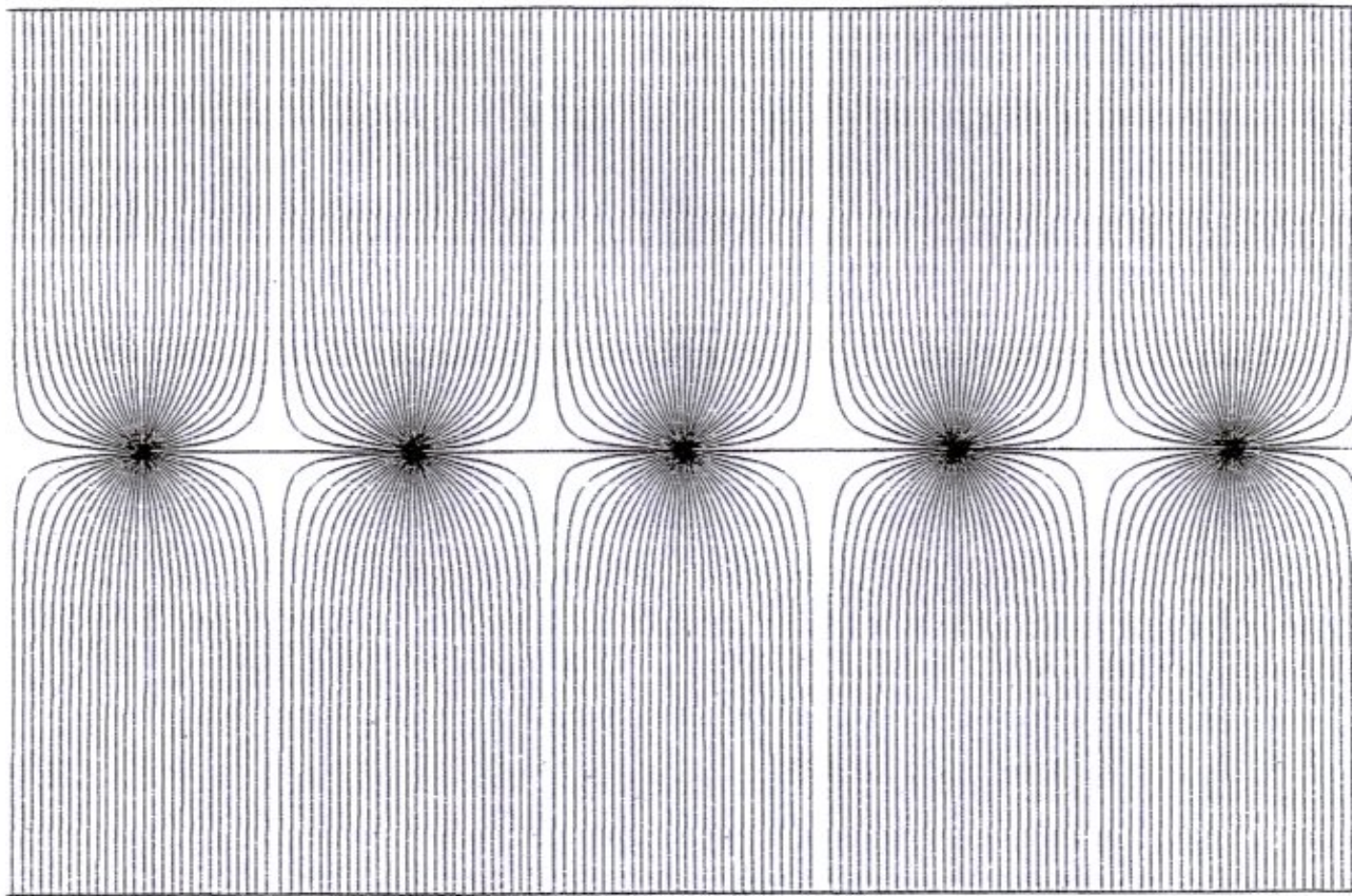
Nobel prize 1992, Rev. Mod. Phys. 65 (1993) 591



allows: tracking of charged particles, some PID capabilities via  $dE/dx$   
large area coverage, high rate capability



as compared to cylindrical arrangement field geometry somewhat different



typical parameters:

$$d = 2 - 4 \text{ mm}$$

$$r_i = 15 - 25 \text{ } \mu\text{m}$$

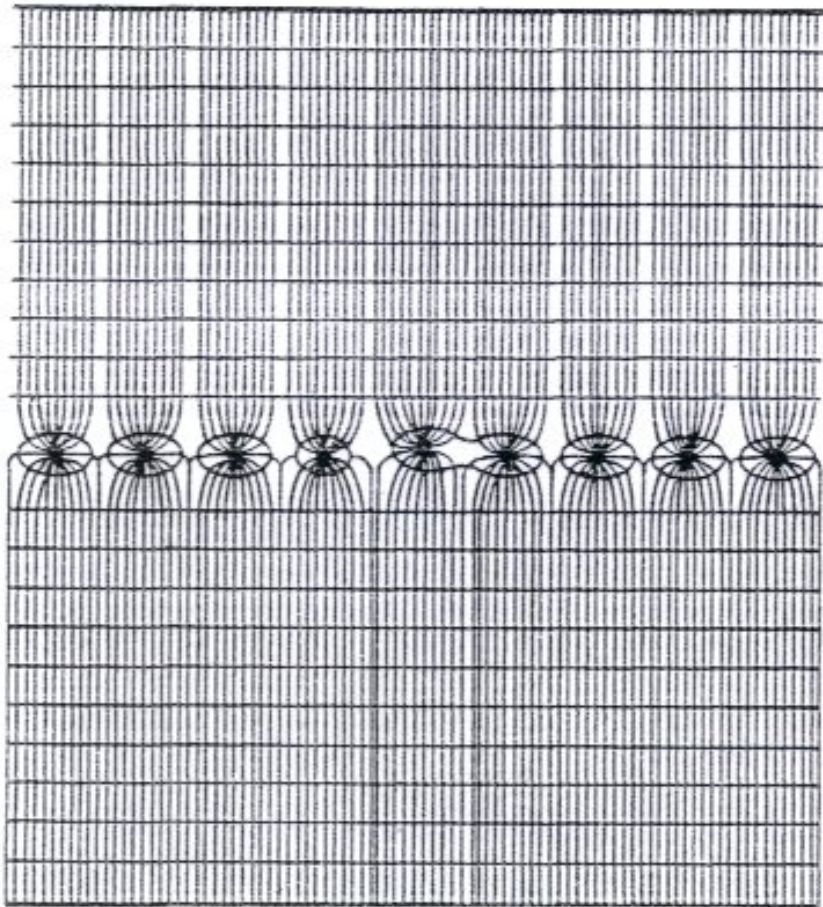
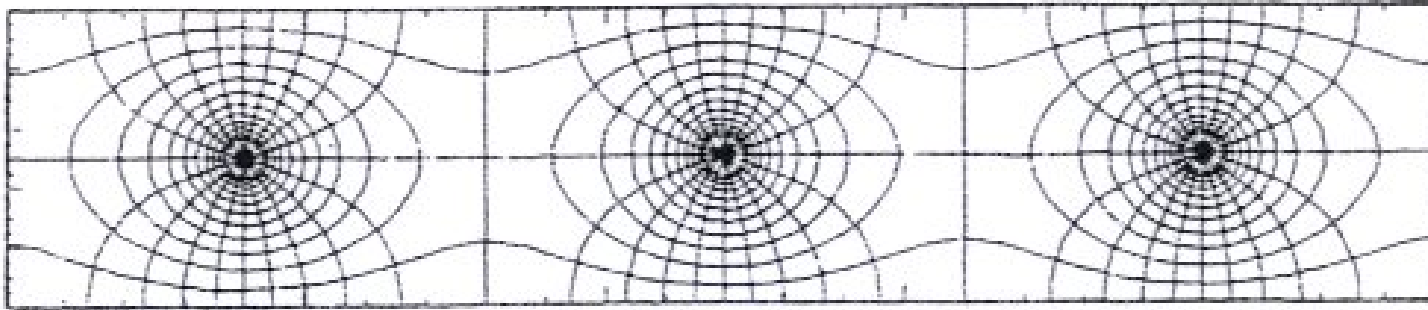
$$L = 3 - 6 \text{ mm}$$

$$U_0 = \text{several kV}$$

total area: many  $\text{m}^2$

typical geometry of electric field lines in multi-wire proportional chamber

in vicinity of anode wire: radial field  
far away homogeneous (parallel-plate capacitor)

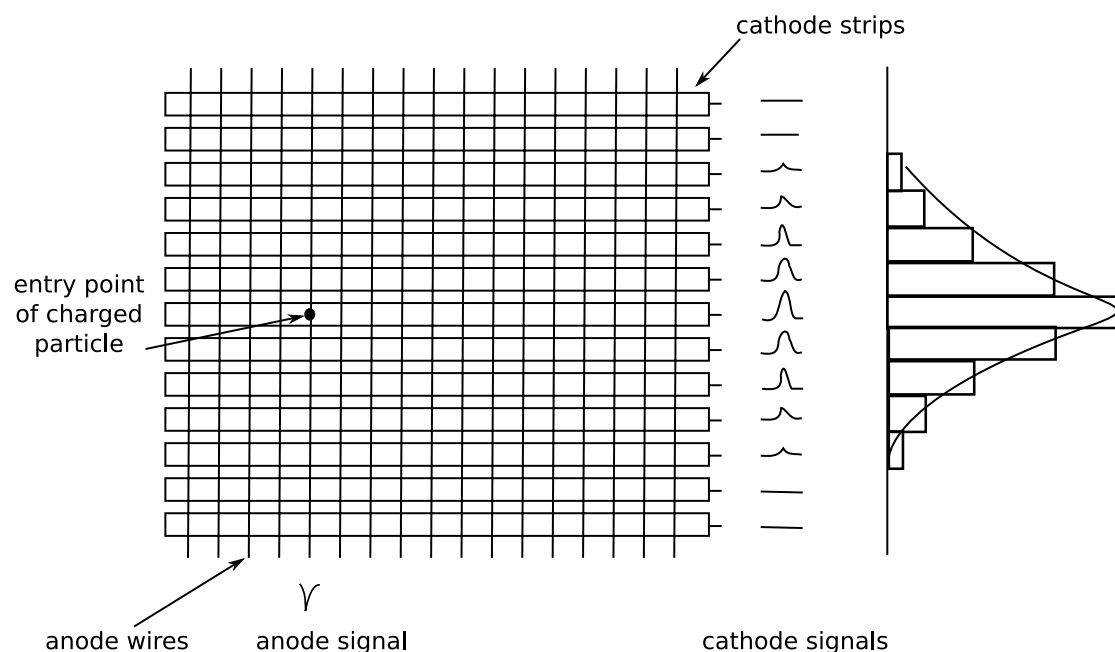


Field lines and equipotential lines

Difficulty:  
even small geometric displacement of an individual wire will lead to effect on field quality.

need of high mechanical precision, both for geometry and wire tension (electrostatic effects and gravitational wire sag, see below)

- electrons from primary and secondary ionization drift to closest anode wire
- in vicinity of wire gas amplification → formation of avalanche  
ends when electrons reach wire or when space charge of positive ions screens electric field below critical value
- signal generation due to electron- and (mostly) slow ion-drift



### typical space point resolution:

since only information about closest wire →

$$\delta_x = d/\sqrt{12} = 577 \mu\text{m for } d = 2 \text{ mm}$$

not very precise and only 1-dimensional

can be improved by segmenting cathode and read-out of induced signal

the center of gravity of signals on cathode strips can be determined with precision of 50...300  $\mu\text{m}$ ! use charge sharing between adjacent strips

Note: The dimension with good resolution is along the wire, perpendicular always  $d/\sqrt{12}$ .



Resolving ambiguities in case of 2 or more hits in one event:  
different orientation of segmentation in several cathode planes

two particles traversing MWPC: with only one orientation of segmentation (strips) possibilities ●● and ○○ cannot be distinguished and one obtains 4 possible coordinates for tracks: 2 real and 2 'ghosts', resolved by second induced strip pattern

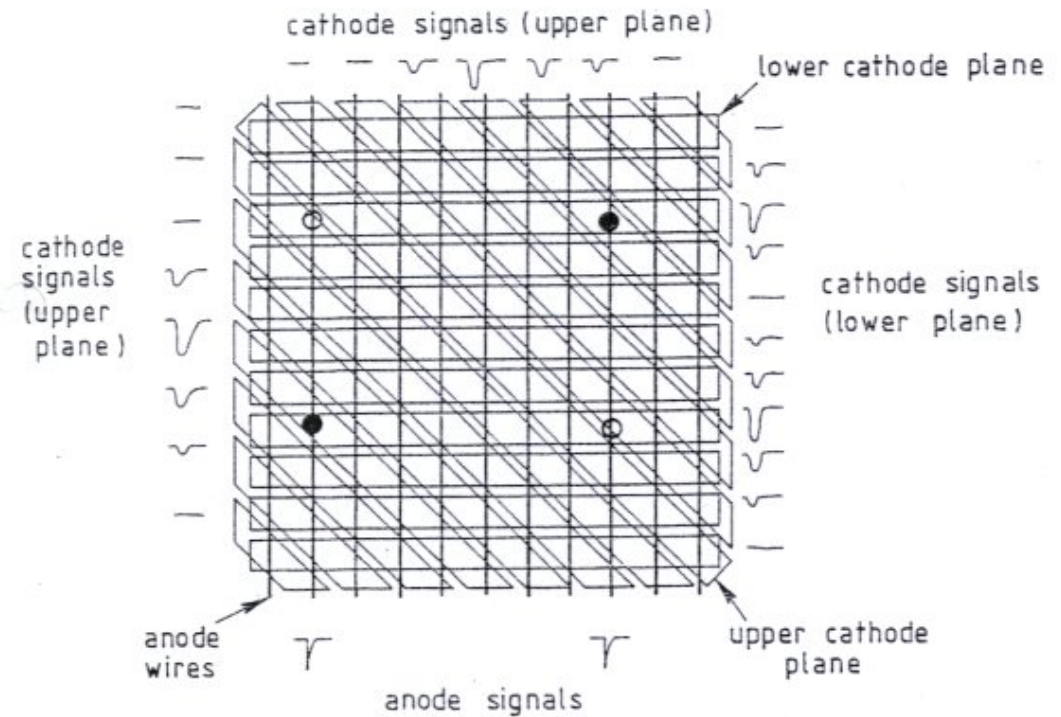
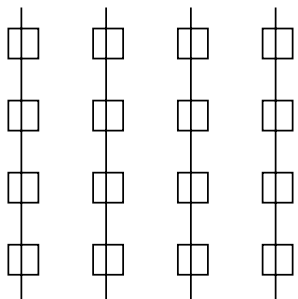


Illustration of the resolution of ambiguities for two particles registered in a multi-wire proportional chamber



for high hit density environment segmentation of cathode into pads truly 2-d measurement.

but: number of read-out channels grows quadratically with area (\$\$)

# Stability of wire geometry I

Can we make resolution better and better by putting wires closer and closer?

practical difficulty in stringing wires precisely closer than 1 mm

fundamental limitations: stability of wire geometry

- electrostatic repulsion between anode wires, in particular for long wires

→ can lead to 'staggering'

to avoid this, the wire tension  $T$  has to be larger than a critical value  $T_0$  given by

$$U_0 \leq \frac{d}{lC} \sqrt{4\pi\epsilon_0 T_0} \quad \text{with} \quad \begin{array}{l} \text{wire length } l \\ \text{wire distance } d \\ \text{capacity per unit length for cylinder } C = \frac{4\pi\epsilon_0}{2 \ln(r_a/r_i)} \end{array}$$

approximation for MWPC with distance anode-cathode  $L \gg d \gg r_i$

$$C = \frac{4\pi\epsilon_0}{2 \left( \frac{\pi L}{d} - \ln \frac{2\pi r_i}{d} \right)}$$

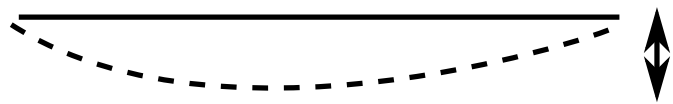
leading to

$$T_0 \geq \left( \frac{U_0 l}{d} \right)^2 4\pi\epsilon_0 \left[ \frac{1}{2 \left( \frac{\pi L}{d} - \ln \frac{2\pi r_i}{d} \right)} \right]^2$$

with  $l = 1 \text{ m}$ ,  $U_0 = 5 \text{ kV}$ ,  $L = 10 \text{ mm}$ ,  $d = 2 \text{ mm}$ ,  $r_i = 15 \text{ } \mu\text{m} \rightarrow T_0 = 0.49 \text{ N } (\simeq 50 \text{ g})$

## Stability of wire geometry II

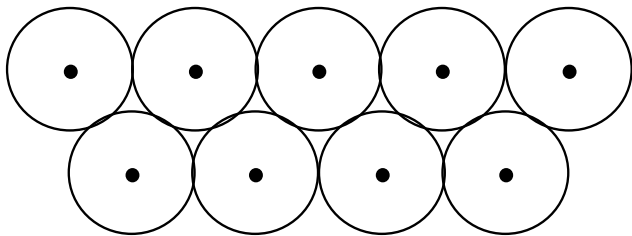
- for horizontal wires also gravity  $\rightarrow$  sag



$$f = \frac{\pi r_i^2}{8} \rho g \frac{l^2}{T} = \frac{m l g}{8 T}$$

gold-plated W-wire  $r_i = 15 \mu\text{m}$ ,  $T$  as above  $\rightarrow f = 34 \mu\text{m} \rightarrow$  visible difference in gain

some of these problems avoided by 'straw tube chambers' (assembly of single-wire proportional counters):



cylindrical wall = cathode  
aluminized mylar foil  
introduced in 1990ies

further big (!) advantage: a broken wire affects only 1 cell, not entire chamber  
straw diameter: 5 – 10 mm, can be operated at over-pressure,  
space point resolution down to  $160 \mu\text{m}$  (e.g. LHCb Outer Tracker)

**short drift lengths:** enable high rates

operation in magnetic field without degradation of resolution

concept employed in several LHC detectors

- can wires be avoided entirely?

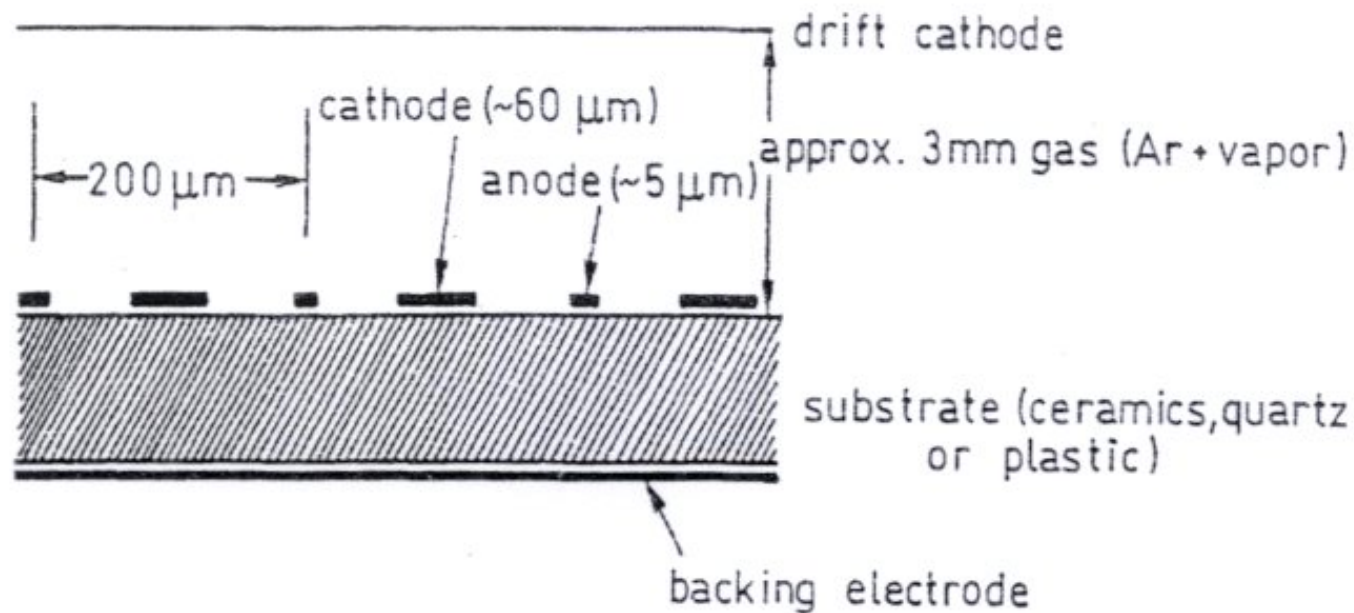
ease of construction

stability

...

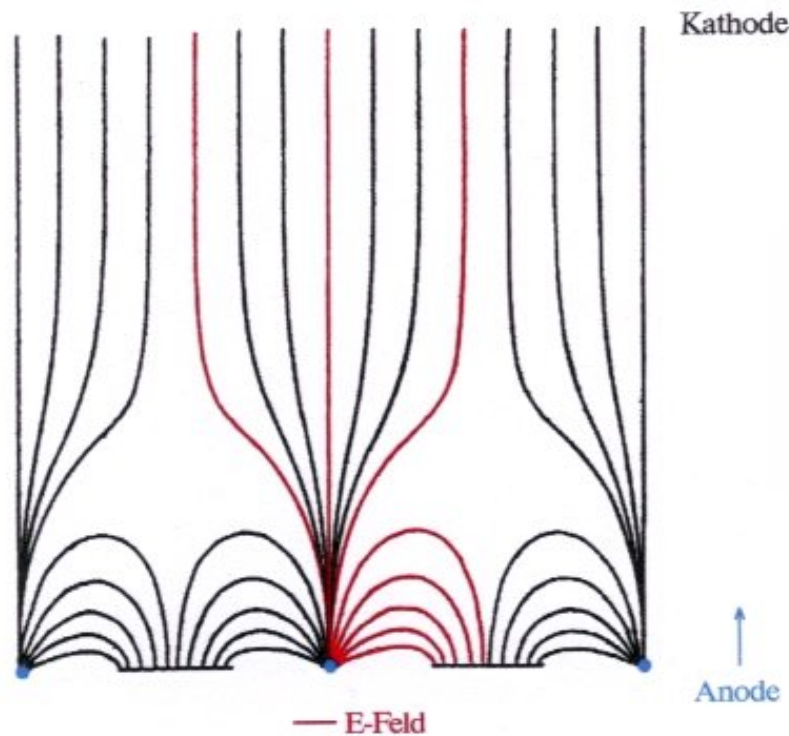
anode can actually be realized by microstructures on dielectrics

*example:* microstrip gas detector (developed in 1990ies)



Schematic arrangement of a microstrip gas detector

## schematics of a **microstrip gas chamber**



directly above anode strip high density of field lines

## *advantages*

- ions drift only 100  $\mu\text{m}$
- high rate capability without build-up of space charge
- resolution

fine structures can be fabricated by electron lithography on ceramics, glass or plastic foil on which a metal film was previously evaporated.

## *problems*

charging of isolation structure

→ time-dependence of gas gain

→ sparks, destruction of anode structure, corrosion of insulator

**basically not a successful concept** - lifetime of detector too limited



# Gas electron multiplier

a possible solution:  
pre-amplification with GEM foil

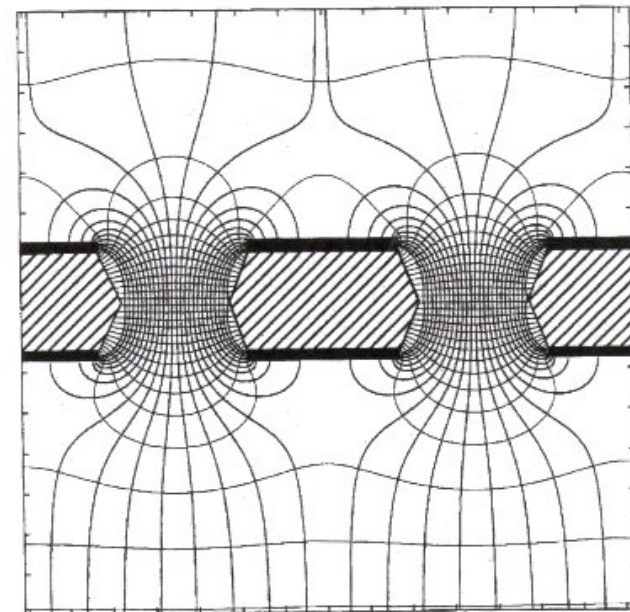
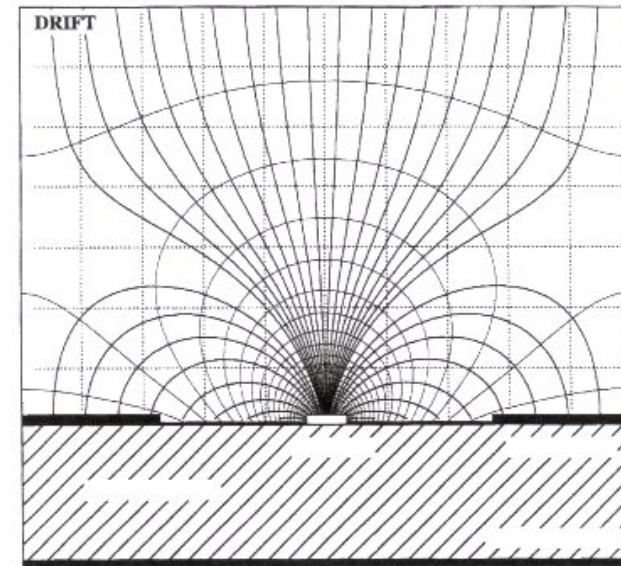
**GEM: gas electron multiplier**

invented by F. Sauli (CERN) ( $\sim 1997$ )

allows reduced electric field  
in vicinity of anode structures.

but: ease of construction again partly  
eliminated and danger of discharge  
on foil (huge capacitance)

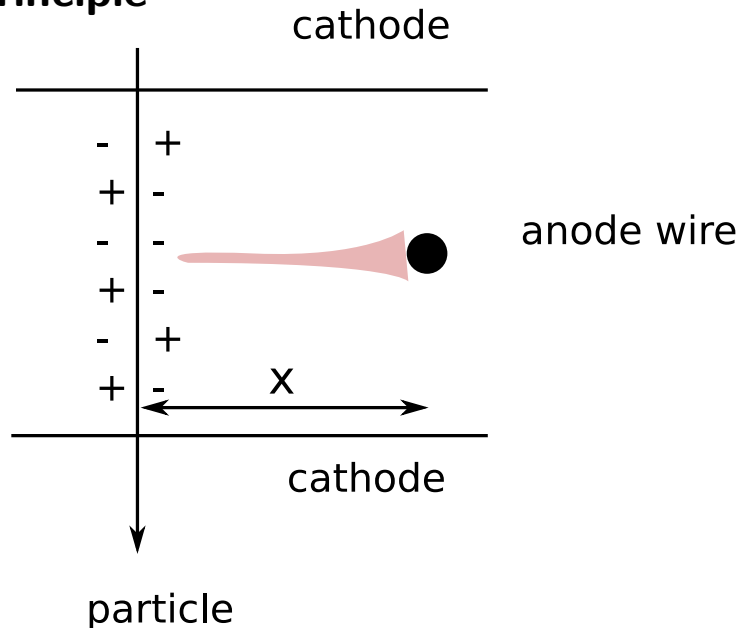
upgrade of Alice TPC for 50 kHz PbPb  
collisions based on quadruple GEM layers  
challenge: to keep ion feedback below 1 %



## 3.6 Drift chambers

invented by A. Walenta, J. Heintze in 1970 at Phys. Inst. U.Heidelberg (NIM 92 (1971) 373)

### Principle



time measurement:

$$x = v_D^- \cdot \Delta t$$

$v_D^-$ : drift velocity of electrons

or, in case drift velocity changes along path

$$x = \int v_D^-(t) dt$$

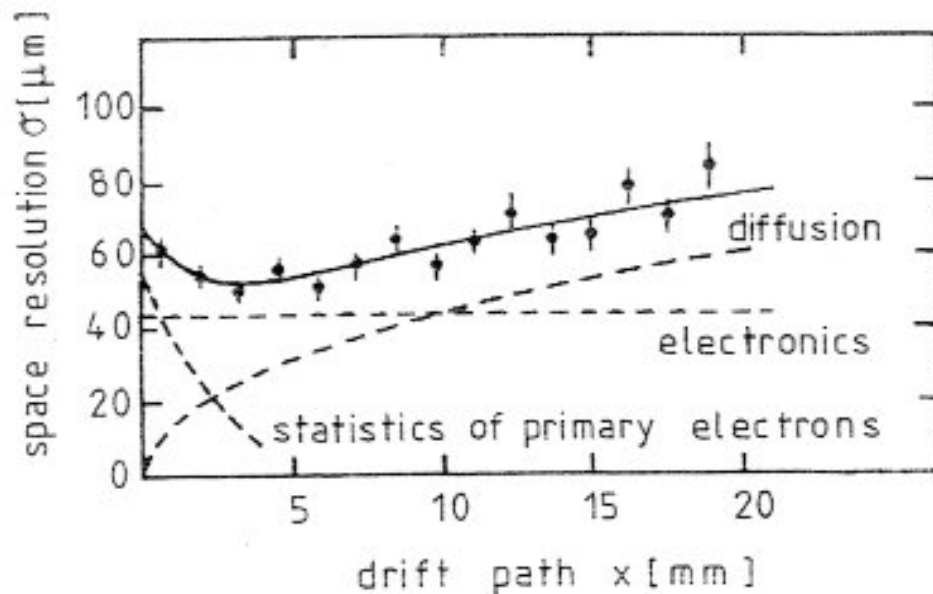
needs well defined drift field → introduce additional field wires in between anode wires.

but: In that case number of anode wires can be reduced in comparison to MWPC at improved spatial resolution

$$\left. \begin{array}{l} v_D^- \simeq 5 \text{ cm}/\mu\text{s} \\ \text{time resolution of front end electronics } \sigma_t \simeq 1 \text{ ns} \end{array} \right\} \sigma_x \simeq 50 \text{ } \mu\text{m} \text{ is possible}$$

but the resolution is affected by diffusion of drifting electrons and statistical fluctuations in primary ionization (in particular in vicinity of wire).

factors affecting spatial resolution in a drift chamber:



spatial resolution in a drift chamber as a function of the drift path

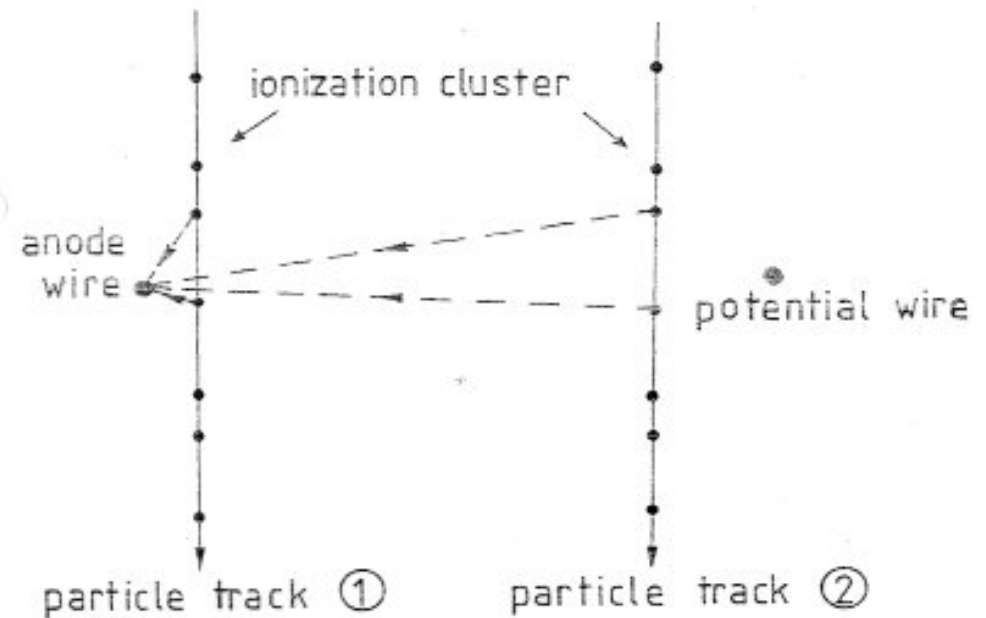
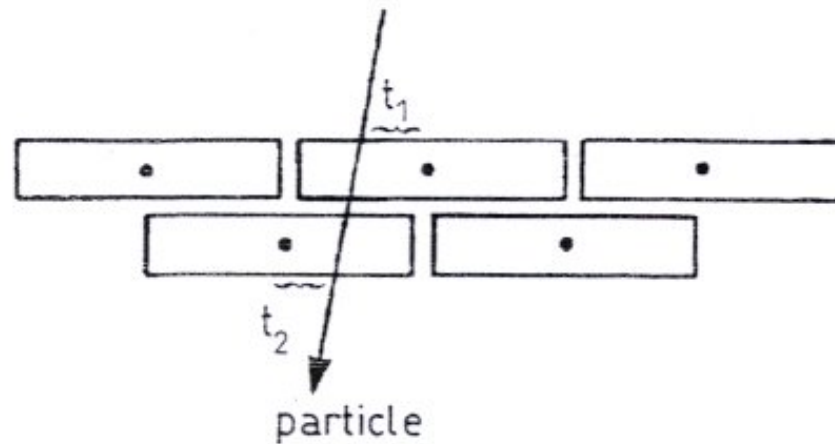


illustration of different drift paths for 'near' and 'distant' particle tracks to explain the dependence of the spatial resolution on the primary ionization statistics

**Difficulty:** time measurement cannot distinguish between particle passing to the left or to the right of the anode wire → 'left-right ambiguity'



resolution of the left-right ambiguity in a drift chamber

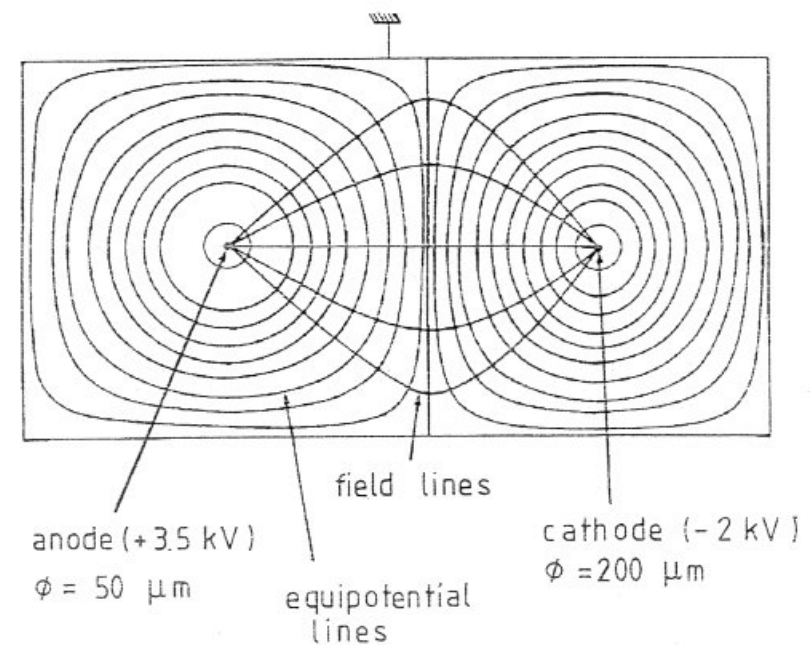
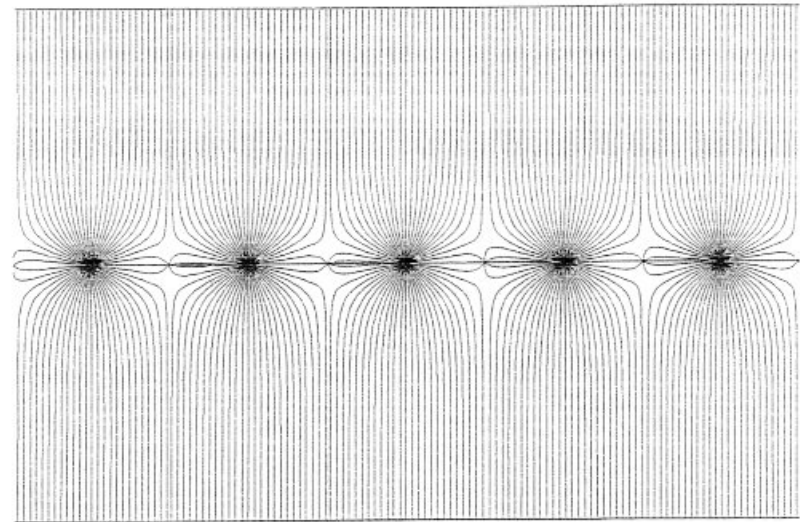
need 2 layers displaced relative to each other by half the wire distance: 'staggered wires'

# How to achieve field quality good enough for drift chamber?

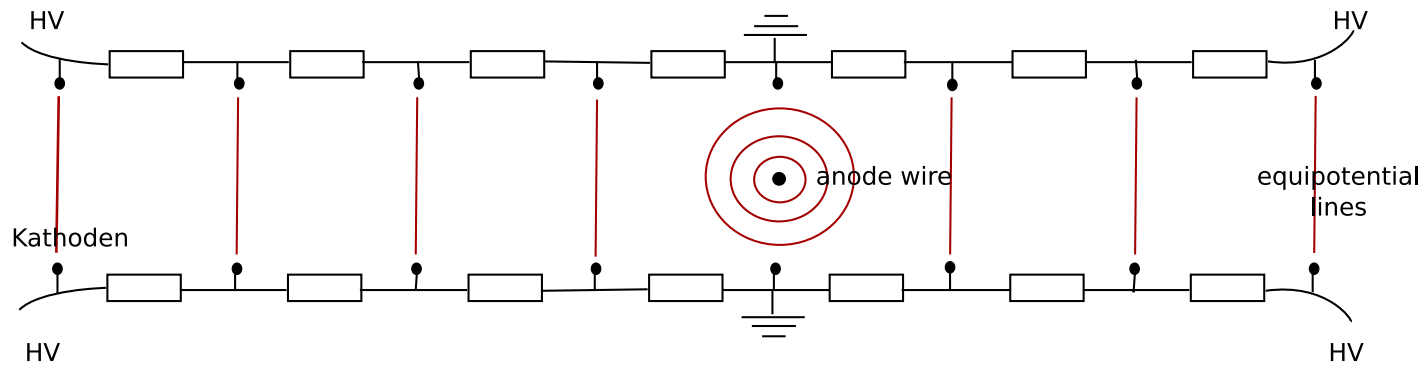
in a MWPC in between anode wires there are regions of very low electric field (see above)

the introduction of additional '**field wires**' at negative potential relative to anode wires strongly improves the field quality

essential for **drift chamber** where **spatial resolution** is determined by **drift time variations** and not by segmented electrode structure



one can build **very large** drift chambers; in this case one introduces a voltage divider by cathode strips connected via resistors, very few or even only one wire.

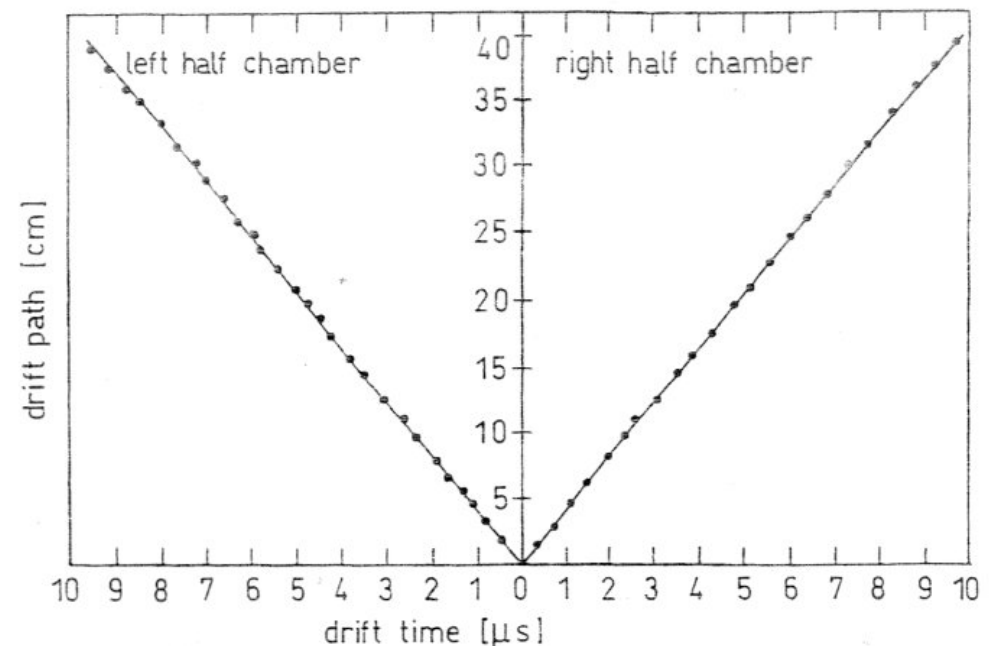


space point resolution limited by mechanical tolerance

for very large chambers  
 $(100 \times 100 \text{ cm}^2) \quad \simeq 200 \text{ } \mu\text{m}$

for very small chambers  
 $(10 \times 10 \text{ cm}^2) \quad \text{even } \simeq 20 \text{ } \mu\text{m}$

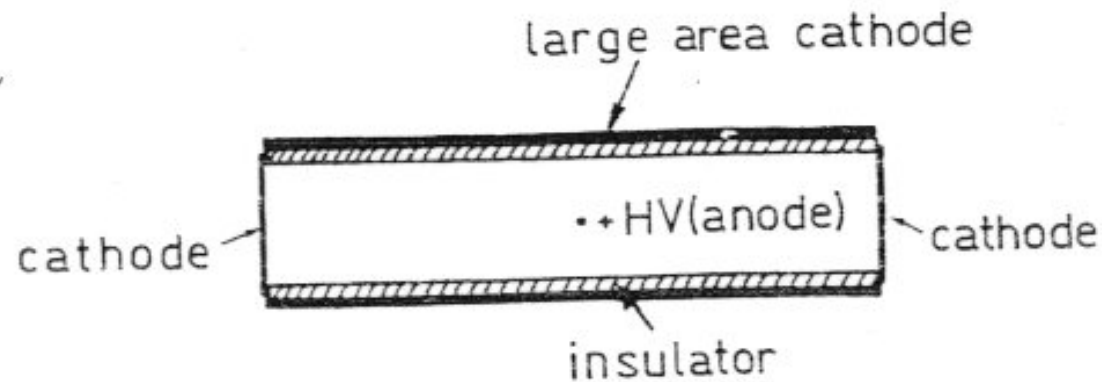
but: hit density has to be low!



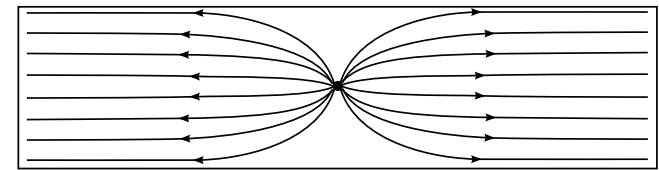
drift time - space relation in a large drift chamber  
 $(80 \times 80 \text{ cm}^2)$  with only one anode wire  
 (Ar + iso-butane 93/7)

field can even be formed by charging up of insulating chamber wall with ions  
after some charging time ions cover insulating layer, no field line end there

### Resistive plate counter:



Principle of construction of an electrodeless drift chamber



After charging the insulating layer with ions



## 3.7 Cylindrical wire chambers

in particular for experiments at storage rings (colliders) to cover maximum solid angle

- initially multi-gap spark chambers, MWPC's
- later cylindrical drift chambers, jet chambers
- today time projection chambers (TPC)

generally these cylindrical chambers are operated in a magnetic field → measurement of radius of curvature of a track → momentum (internally within one detector)

$$p \text{ (GeV/c)} = 0.3 \cdot B \text{ (T)} \cdot \rho \text{ (m)}$$

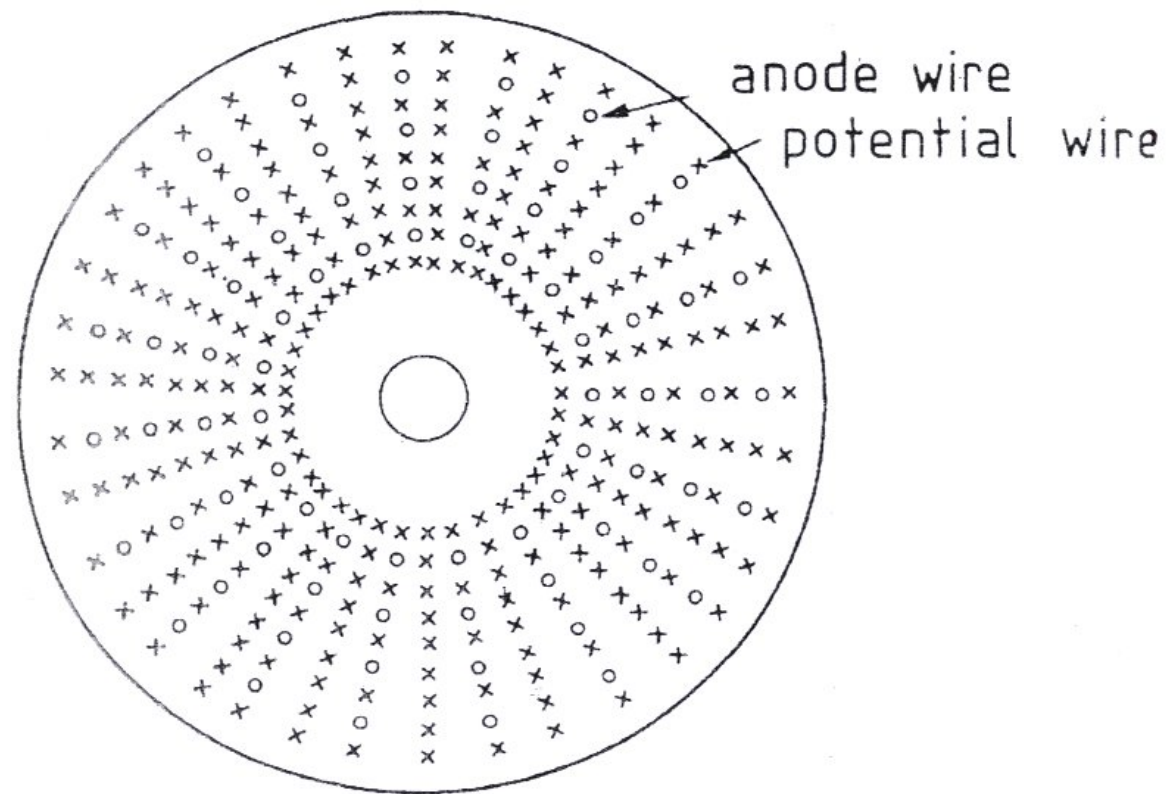


# Principle of a cylindrical drift chamber I

principle of a cylindrical drift chamber: wires in axial direction (parallel to colliding beams and magnetic field)

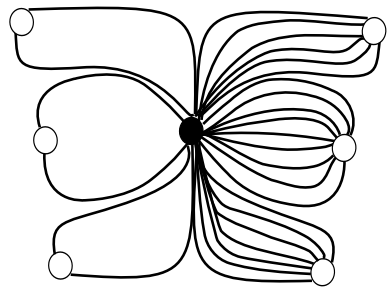
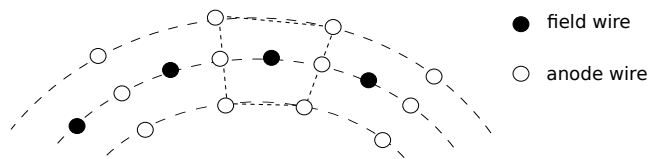
alternating anode and field wires

- one field wire between 2 anode wires
- cylindrical layers of field wires between layers of anode wires → nice drift cells

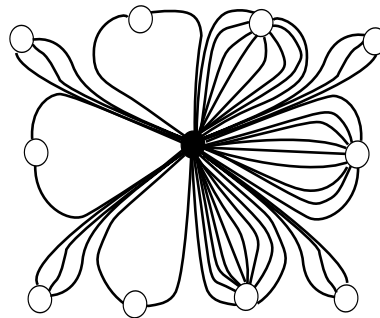
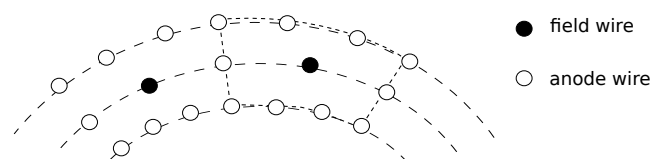


# Principle of a cylindrical drift chamber II

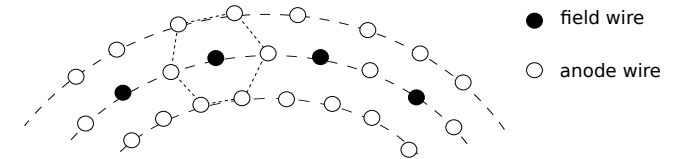
different drift cell geometries:



open drift cell



closed drift cell



also hexagonal drift cell

always thin anode wires ( $\varnothing \simeq 30 \mu\text{m}$ ) and thicker field wires ( $\varnothing \simeq 100 \mu\text{m}$ ), generally field quality better for more wires per drift cell, but:

- more labor-intensive construction
- wire tension enormous stress on end plates, e.g. for chamber with 5000 anode and 15000 field wires  $\rightarrow$  2.5 t on each endplate

## Determination of coordinate along the wire

- current measurement on both ends of anode wire  
charge division, precision about 1% of wire length

$$z \propto \frac{l_1 - l_2}{l_1 + l_2}$$

- time measurement on both ends of wire
- 'stereo wires': layer of anode wires inclined by small angle  $\gamma$  ('stereo angle')  
 $\rightarrow \sigma_z = \sigma_x / \sin \gamma$

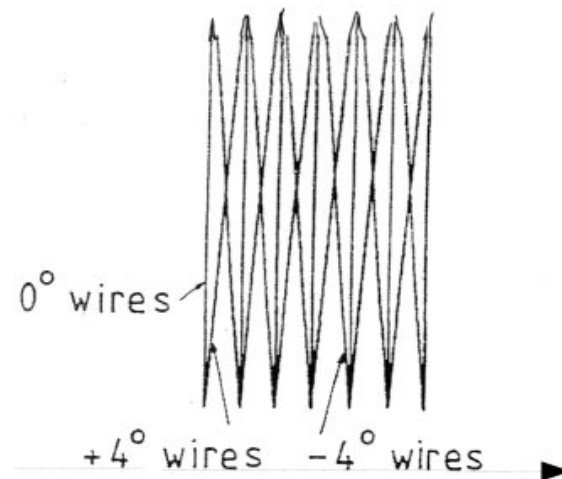
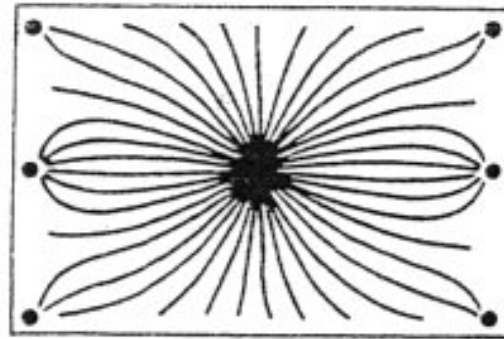
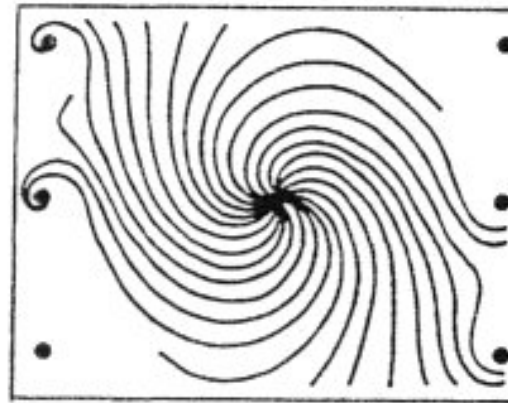


illustration of the determination of the coordinate along the anode stereo wires

in general drift field  $E$  perpendicular to magnetic field  $B \rightarrow$  Lorentz angle for drifting charges



(a)

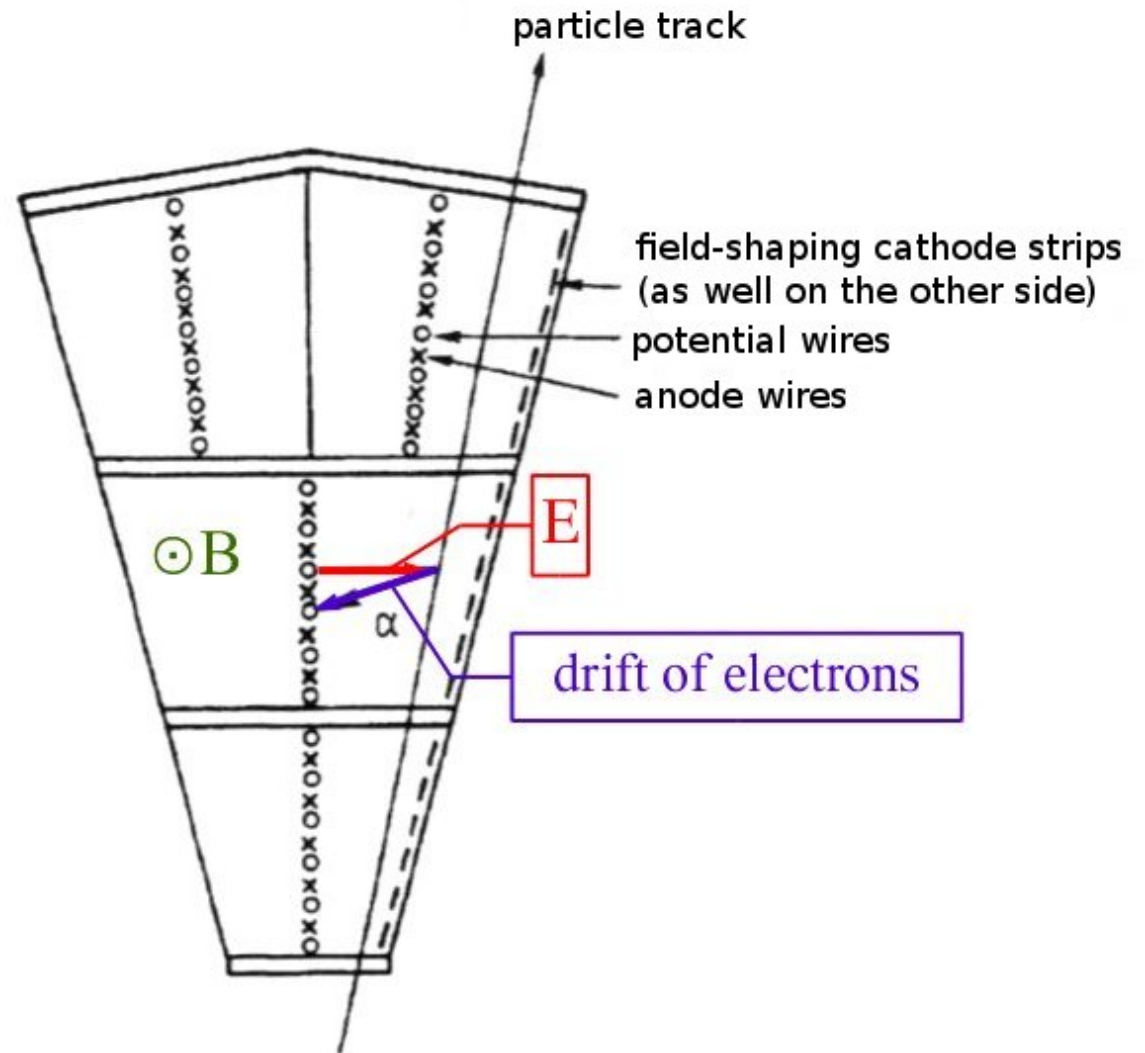


(b)

drift trajectories in an open rectangular drift cell a) without and b) with magnetic field

## 3.8 Jet drift chambers

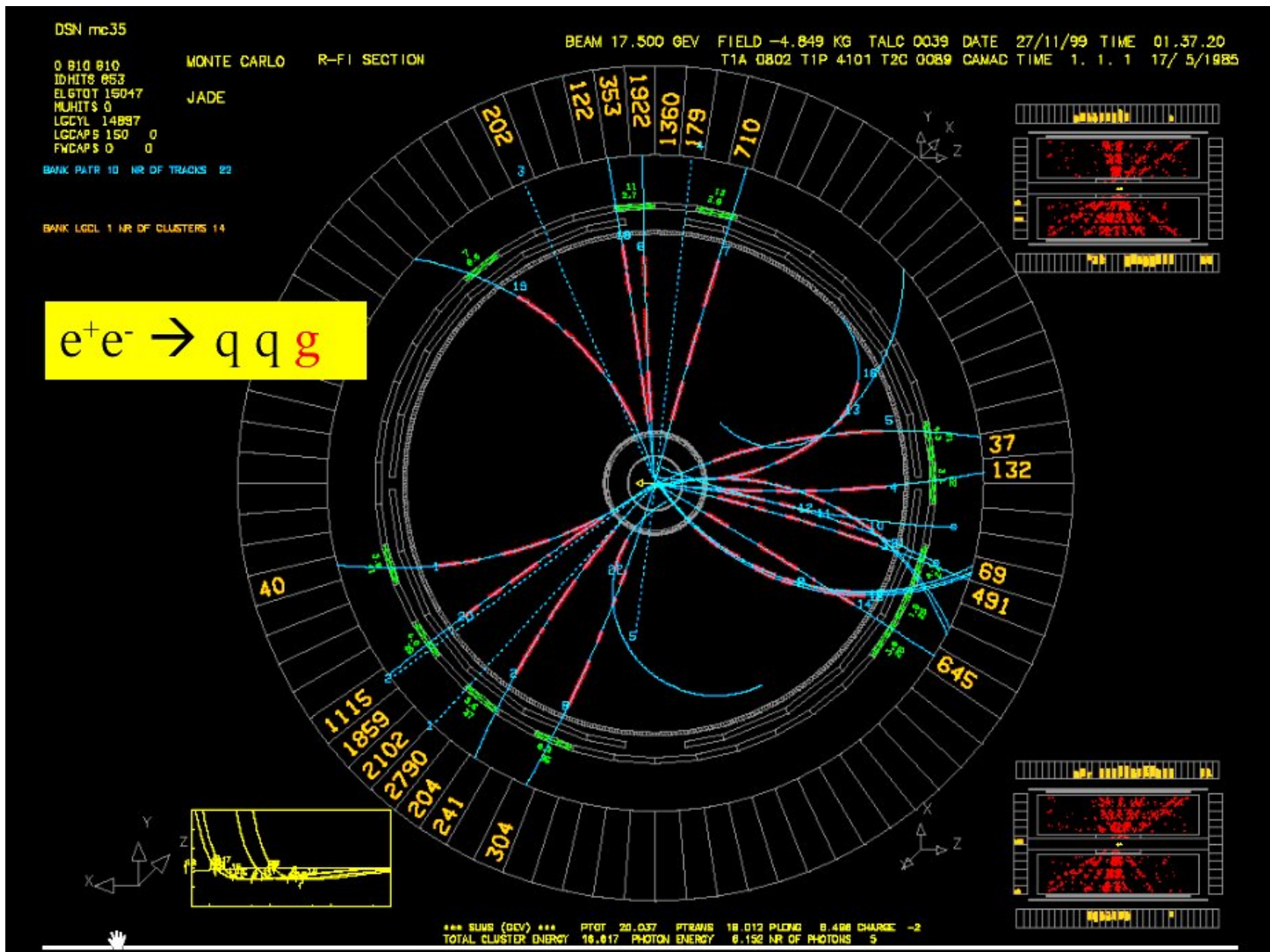
large drift cells  
optimize number of measurements per track  
(typically 1/cm)



example: JADE jet chamber for PETRA, built by J.Heintze et al. Phys. Inst. U. Heidelberg  
length: 2.34 m, radial track length: 57 cm, 47 measurements per track  
 $\sigma_{r\phi} = 180 \mu\text{m}$ ,  $\sigma_z = 16 \text{ mm}$





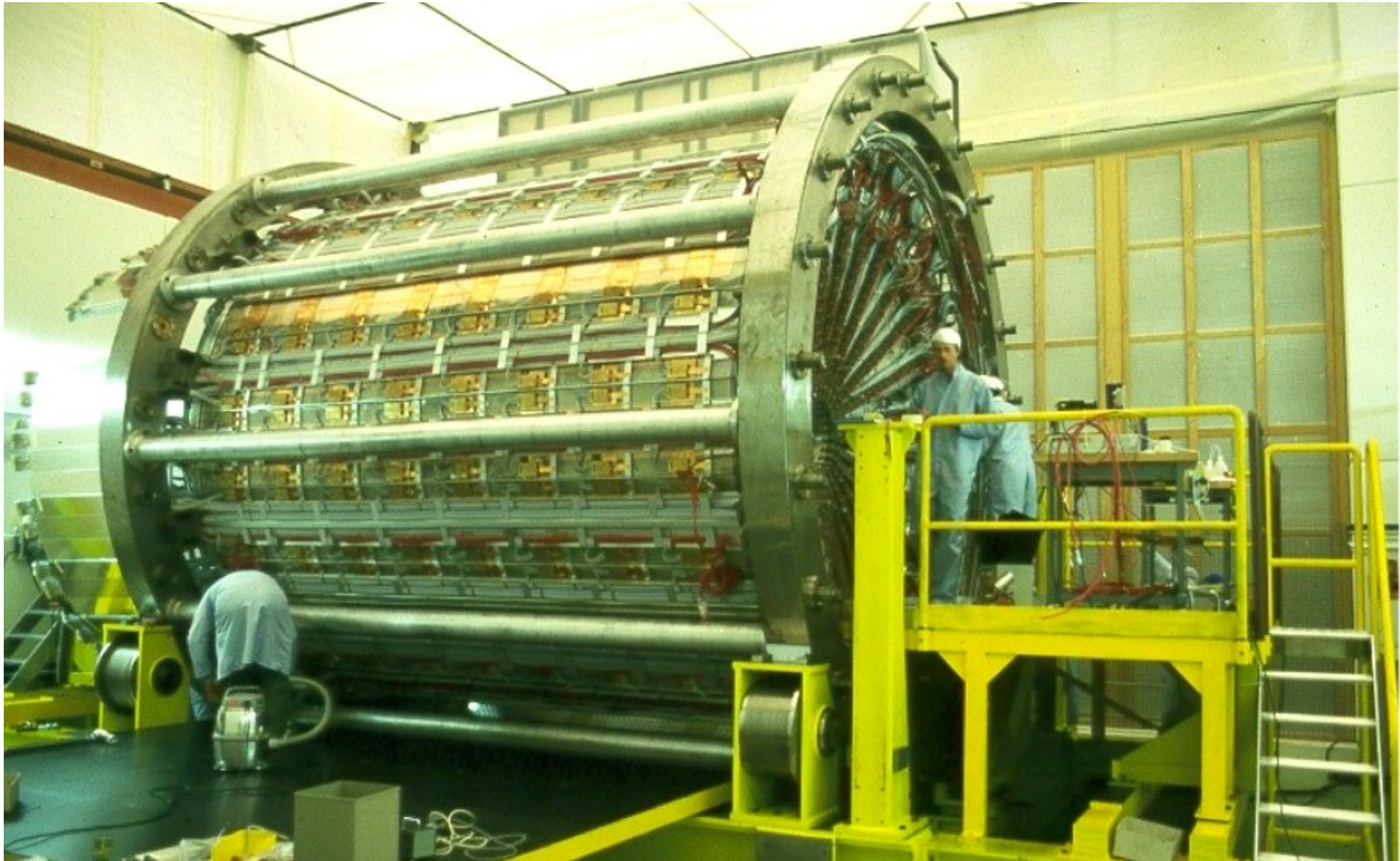


3-jet event by JADE – measurements taken at PETRA → discovery of gluon

another example: OPAL at CERN LEP: central tracking chamber built by team from Phys. Inst. Heidelberg – Heintze, Wagner, Heuer, ...

length: 4 m, radius: 1.85 m, 159 measurements per track, gas: Ar/CH<sub>4</sub>/C<sub>4</sub>H<sub>10</sub> at 4 bar

$\sigma_{r\phi} = 135 \mu\text{m}$ ,  $\sigma_z = 60 \text{ mm}$

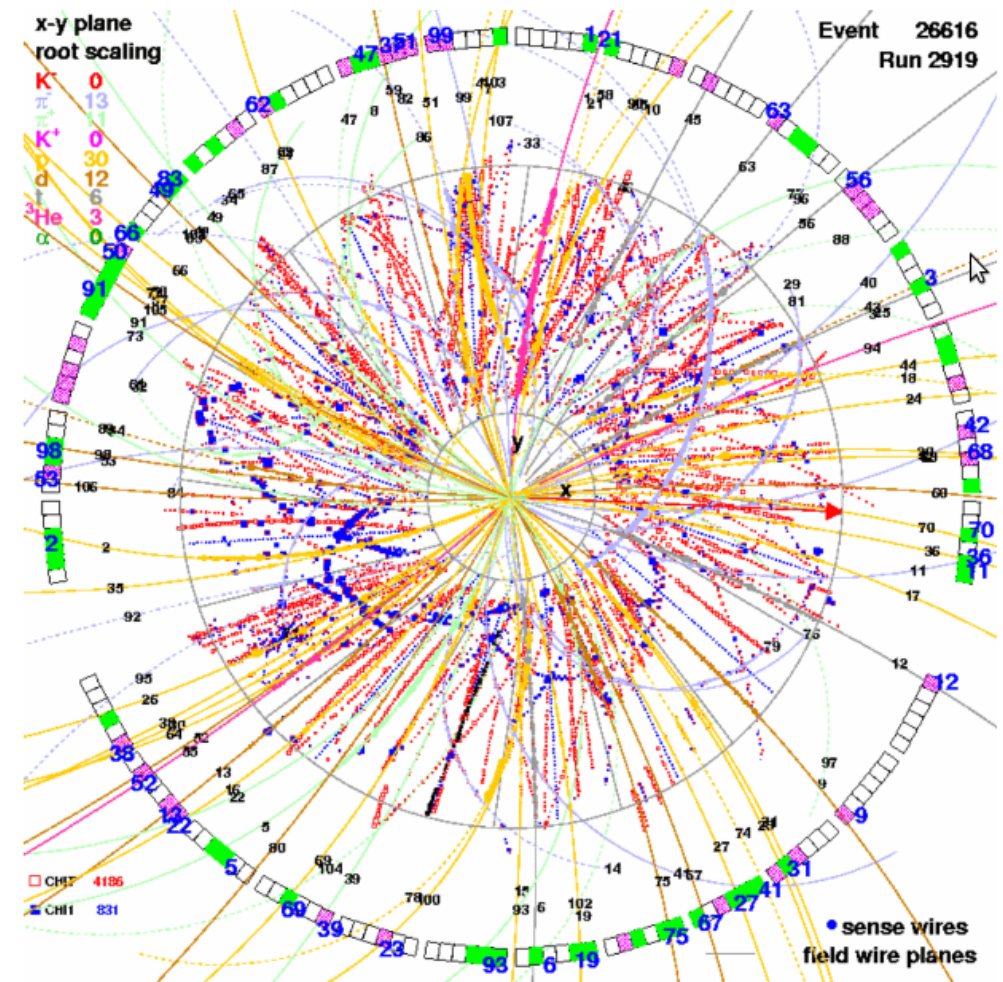
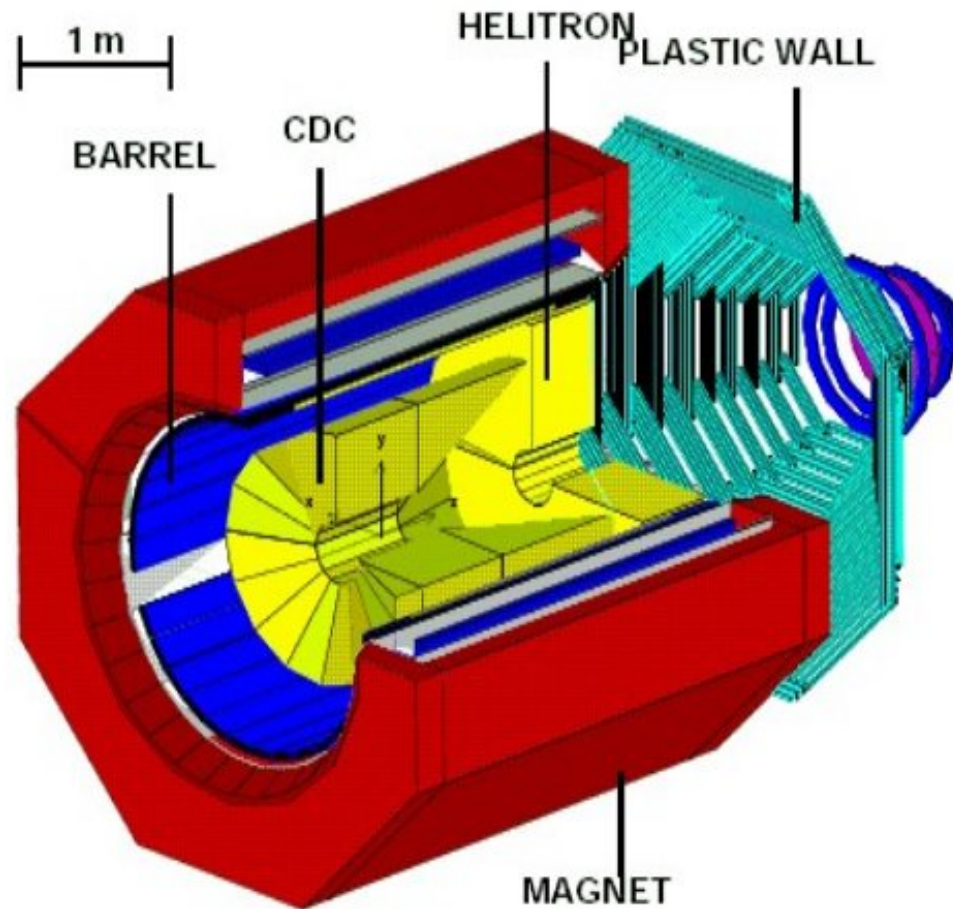




## interior of jet chamber of OPAL



application for heavy ion collisions: FOPI (experiment at SIS at GSI):  
central drift chamber (CDC), D. Pelte and N. Herrmann Phys. Inst. U.Heidelberg





## 3.9 Time Projection Chamber TPC

3-dimensional measurement of a track – ‘electronic bubble chamber’  
invented by D. Nygren in 1974 at Berkeley

(mostly) cylindrical detector

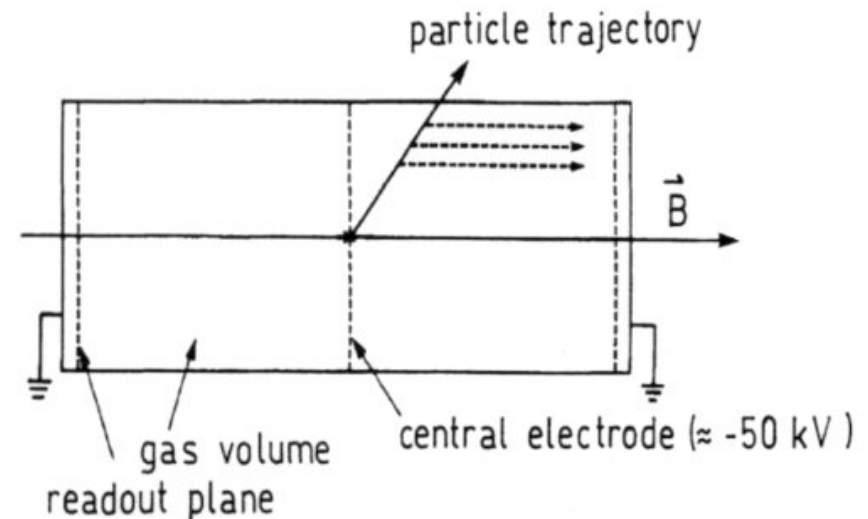
central HV cathode

MWPCs at the endcaps of the cylinder

electrons drift in homogenous electric fields

towards MWPC, where **arrival time and point  
and amount of charge are continuously sampled**  
(flash ADC)

generally with  $B \parallel E \rightarrow$  Lorentz angle = 0



Working principle of a TPC

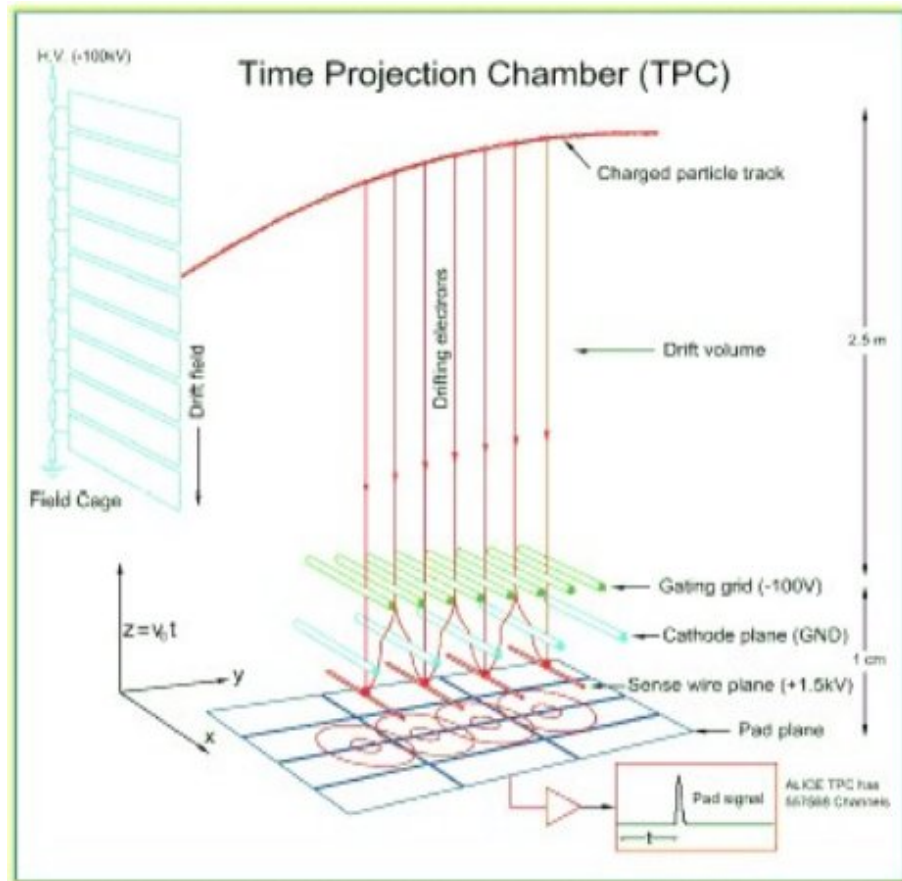
advantages:

- complete track determination within one detector  $\rightarrow$  good momentum measurement
- relatively few wires (mechanical advantage)
- since also charge is measured: particle identification via  $dE/dx$
- drift parallel to  $B \rightarrow$  transverse diffusion suppressed by factors 10 – 100 (see above)

disadvantages

- drift time: relatively long - tens of microseconds  $\rightarrow$  not a high rate detector
- large data volume

## principle of operation of a TPC



continuously sample induced charge or current signals in a MWPC at end of long drift path

z-dim given by drift time

x-dim given by charge sharing of cathode pads

y-dim given by wire/pad number

truly 3-dimensional measurement of ionization points of entire track and in fact of many tracks simultaneously

typical resolution:

z: mm

$r\phi$  or  $x$ : 150–300  $\mu\text{m}$

y: mm

$dE/dx$ : 5 – 10%, trick:

kill Landau tail by evaluating truncated mean

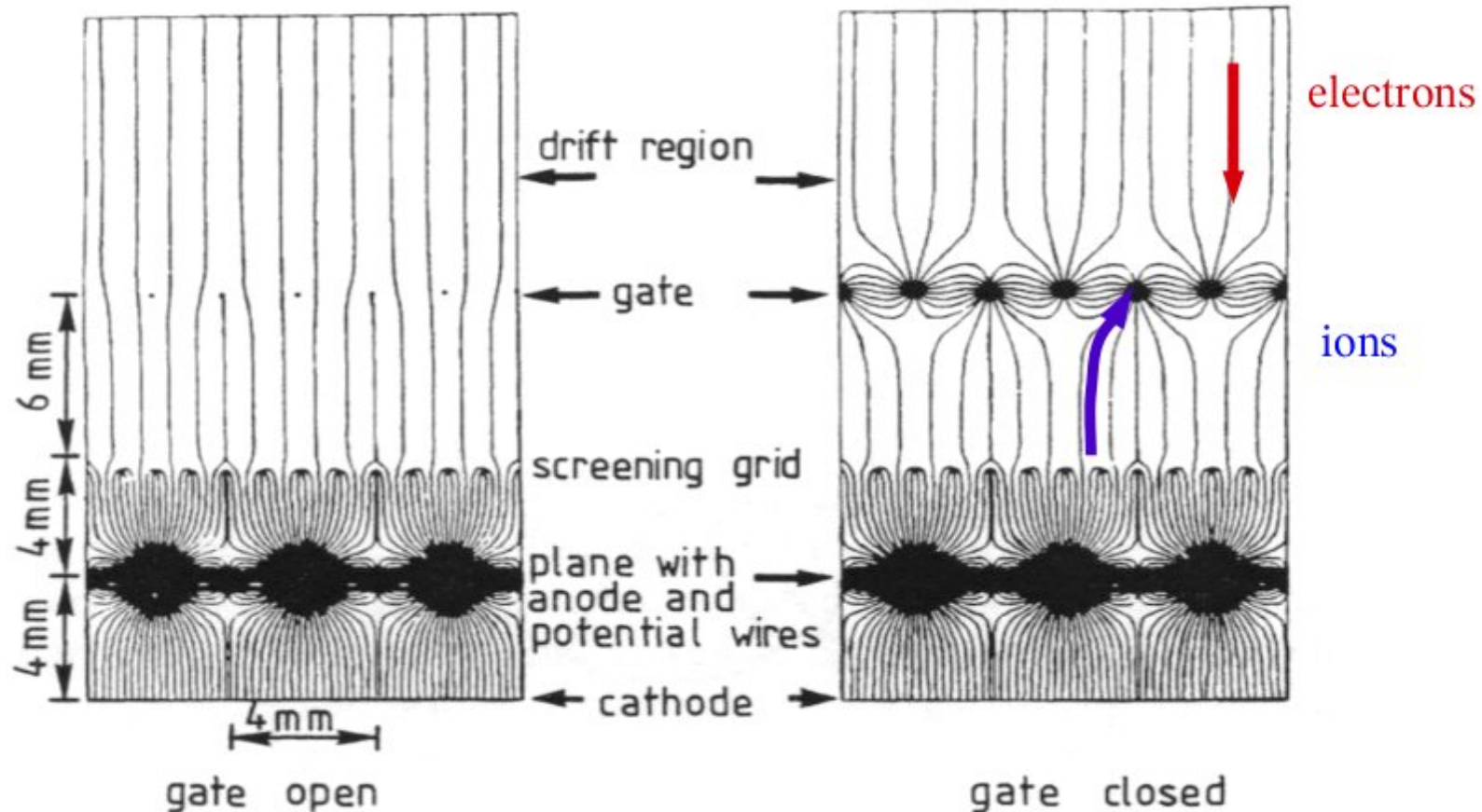
challenges:

- long drift path (attachment, diffusion, baseline)
- large volume (precision)
- large voltages (discharges)
- extreme load in Pb+Pb collisions
  - space charge in drift volume
  - leads to distortion of  $\vec{E}$
  - gating grid opened (fast  $\sim 1 \mu\text{s}$ ) for triggered events only, otherwise opaque ( $\pm\Delta V$ )

**serious difficulty:**

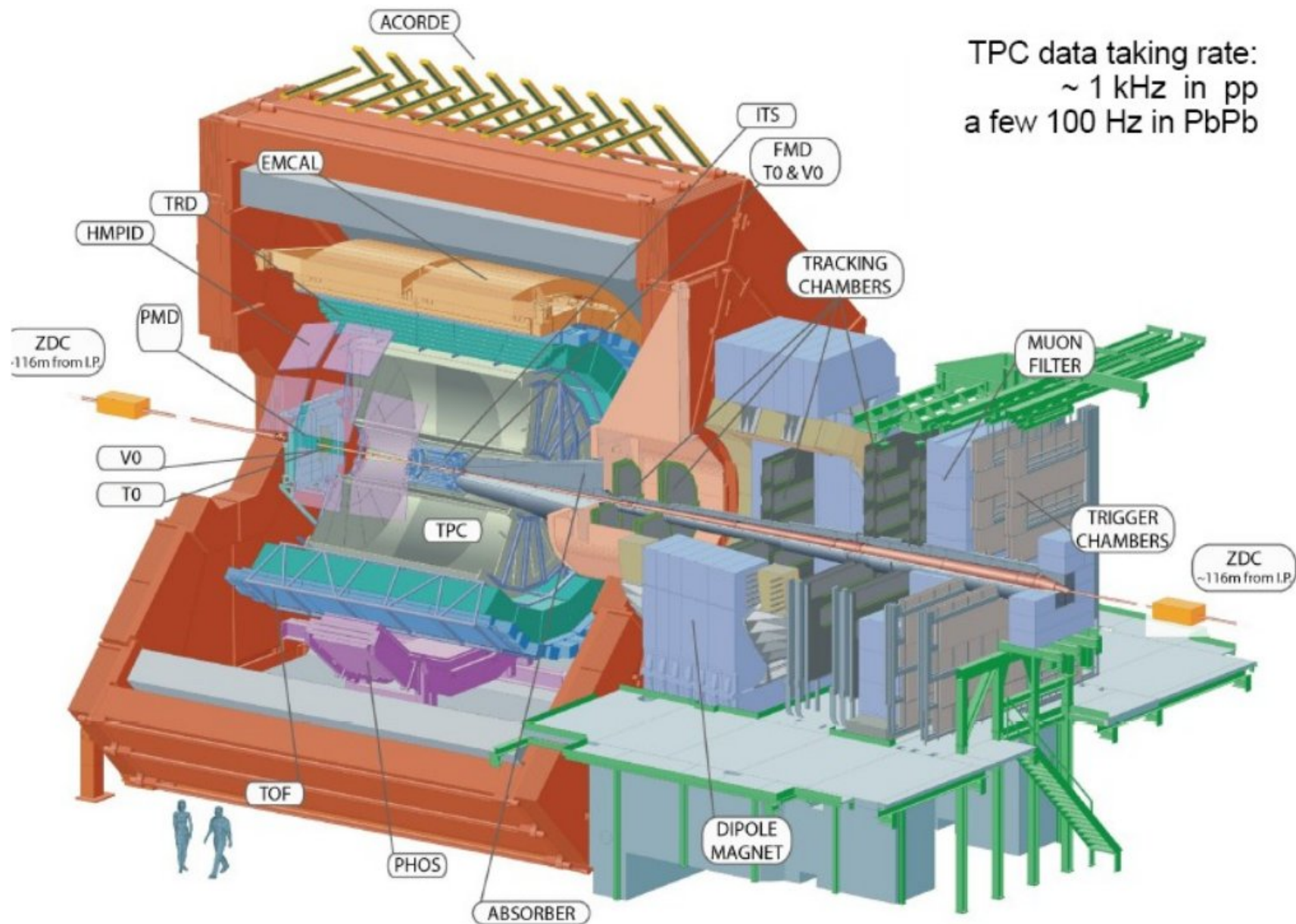
**space charge effects** since also ions have long drift path and move factor 1000 more slowly, positive ions change effective E-field in drift region, most (5000:1) come from amplification region

**trick:** invention of gating grid



upon interaction trigger switch gating grid to 'open' for max drift time, then close again  
 → all ions from amplification drift toward gating grid and do not enter drift region.

# example: the ALICE TPC for LHC Pb + Pb collisions

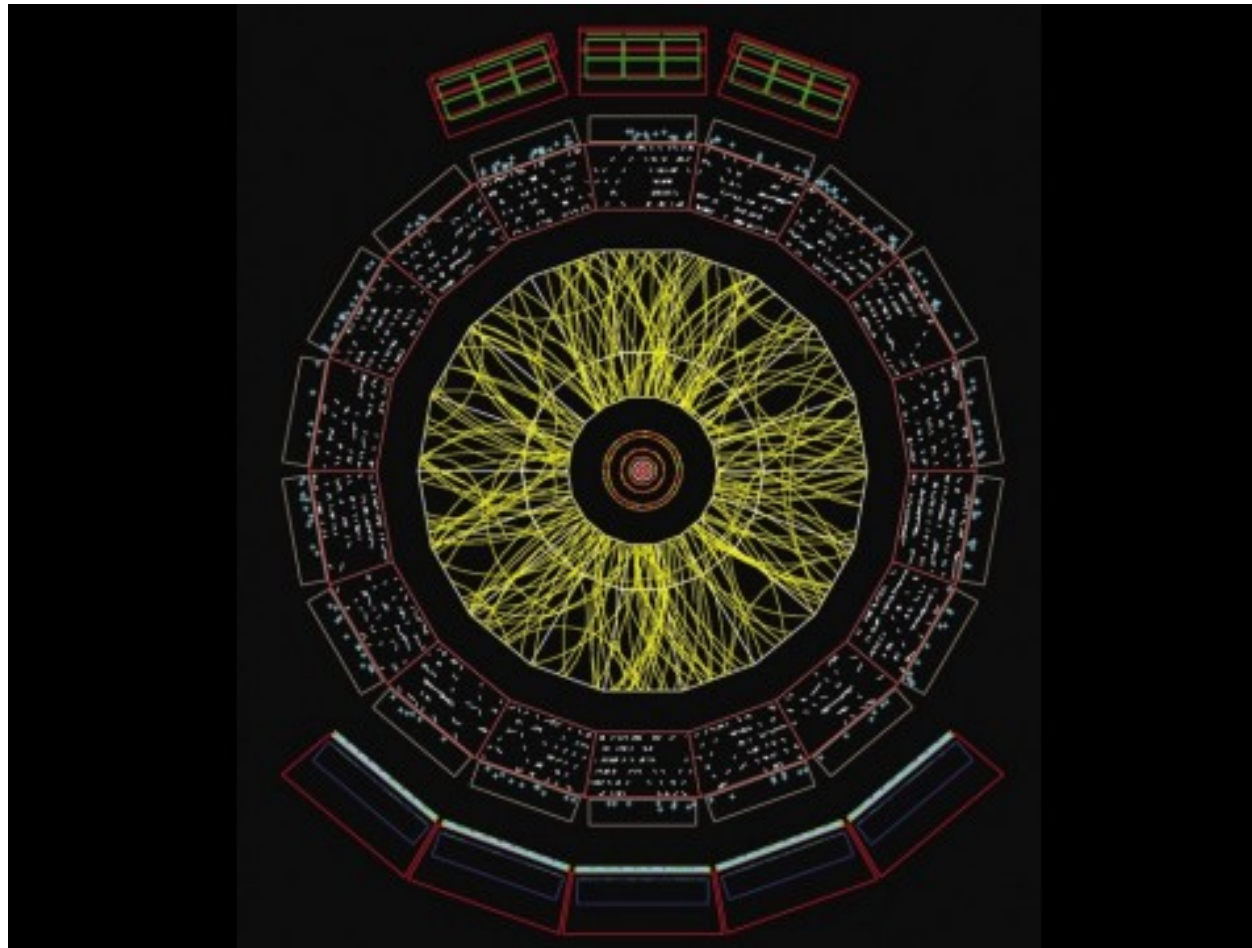




## example: the ALICE TPC for LHC Pb + Pb collisions

the challenge:

identification and reconstruction of 5000 (up to 15000) tracks of charged particle in one event



cut through central barrel of ALICE:  
tracks of charged particles in a 1 degree segment in  $\theta$  (1% of all tracks)

## example: the ALICE TPC for LHC Pb + Pb collisions

### challenges:

- very high multiplicity and desire for very good resolution
  - space charge
    - optimize gating grid (even 1% leakage would be deadly)
    - rate limitation, good luminosity monitoring
  - occupancy, want to keep it at inner radius below 40%
    - optimize pad sizes and shapes ( $4 \times 7.5$  mm, total 558 000)
    - 1000 time samples, 159 samples radially
- momentum resolution
  - low multiple scattering, small diffusion
    - low Z cold gas Ne/CO<sub>2</sub> coupled with small drift cells (occupancy)  
temperature control to 0.1 K (even resistors need to be cooled)  
need to know electric field to  $10^{-4}$  precision
    - small amount of electron-ion pairs
    - high gas gain of 10000
- event rate
  - limited by drift time (cold gas and not more than 100 kV, 90  $\mu$ s)
  - data volume (1 central collision 60 MByte, can't store much more than a few GByte/s)

### technical specs:

$r = 0.85 - 2.47$  m, length  $2 \times 2.5$  m, material budget  $3.5\% X_0$

### approximate performance:

$\sigma(p)/p = 1\%$   $p$ , efficiency 97%,  $\sigma_{dE/dx}/(dE/dx) \leq 6\%$ , 100-200 Hz event rate



inside the field cage:





# The TPC (Time Projection Chamber) – 3D reconstruction of up to 15 000 charged particle tracks per event

**with 95 m<sup>3</sup> largest TPC ever built**

central HV electrode 100 kV

field cage: voltage divider with E-field homogeneity of  $10^{-4}$

in the end caps: 72 multi-wire proportional chambers with cathode pad read-outs



**560 million pixels!**

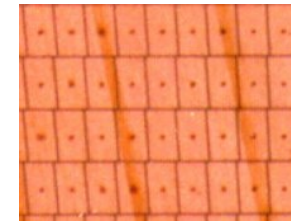
precision better than 500  $\mu\text{m}$  in all 3 dimensions,  
159 points per track

# Construction of multi-wire proportional chambers, 3 wire planes plus cathode pad read-out

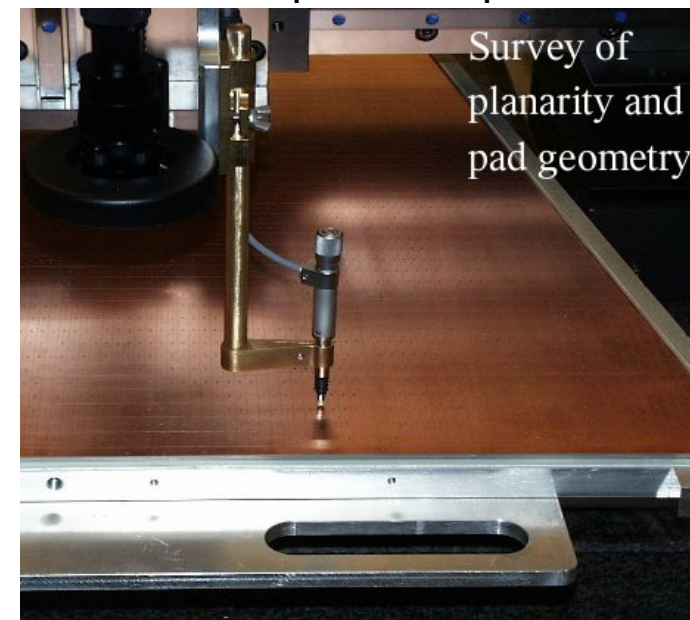
at GSI, Phys. Inst. U. Heidelberg. U. Bratislava

challenge: small spacings, high gas gain, high geometrical precision

Pad Plane: 5504 pads ( $4 \times 7.5$  mm)

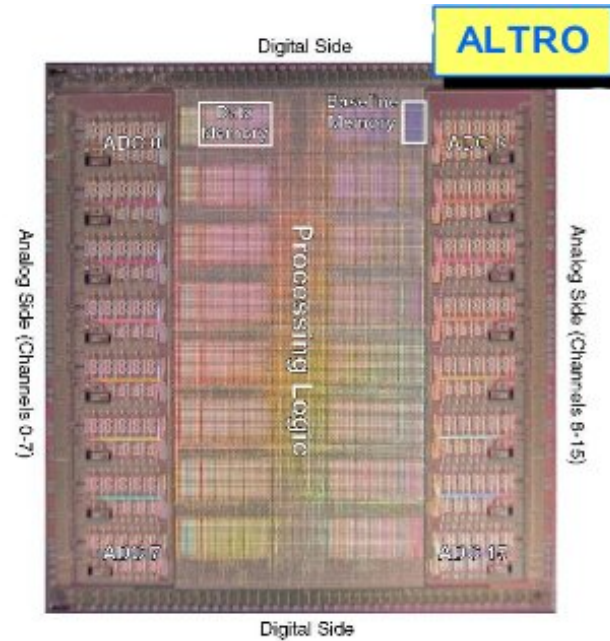
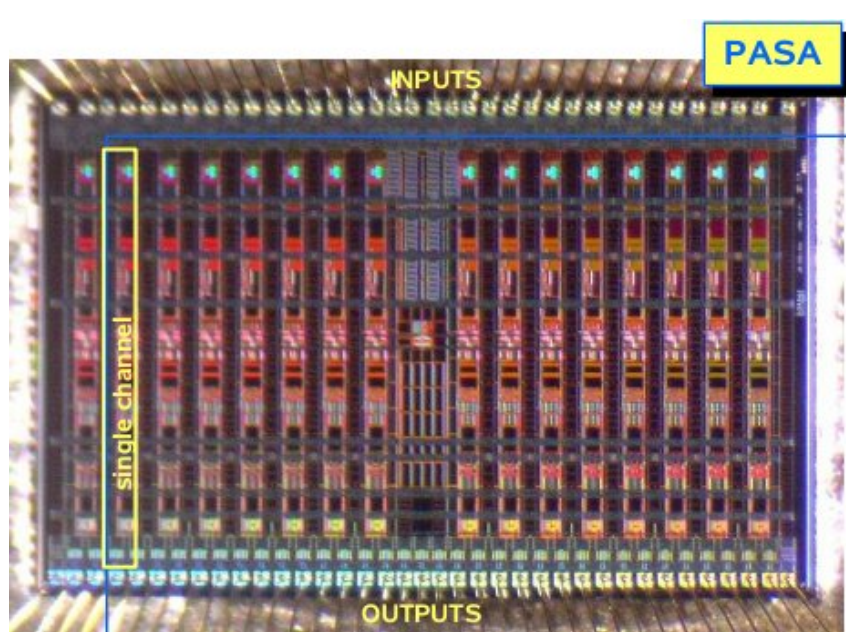


Close-up on the pads





# TPC Front End Electronics – 2 ASICS developed at Phys. Inst. U.Heidelberg and CERN, cooperation with ST Microelectronics



excellent performance  
(now also used by  
STAR at RHIC)

PASA: low noise preamplifier/shaper

ALTRO: commercial ADC (ST)  
**in same custom chip** with digital signal  
processing

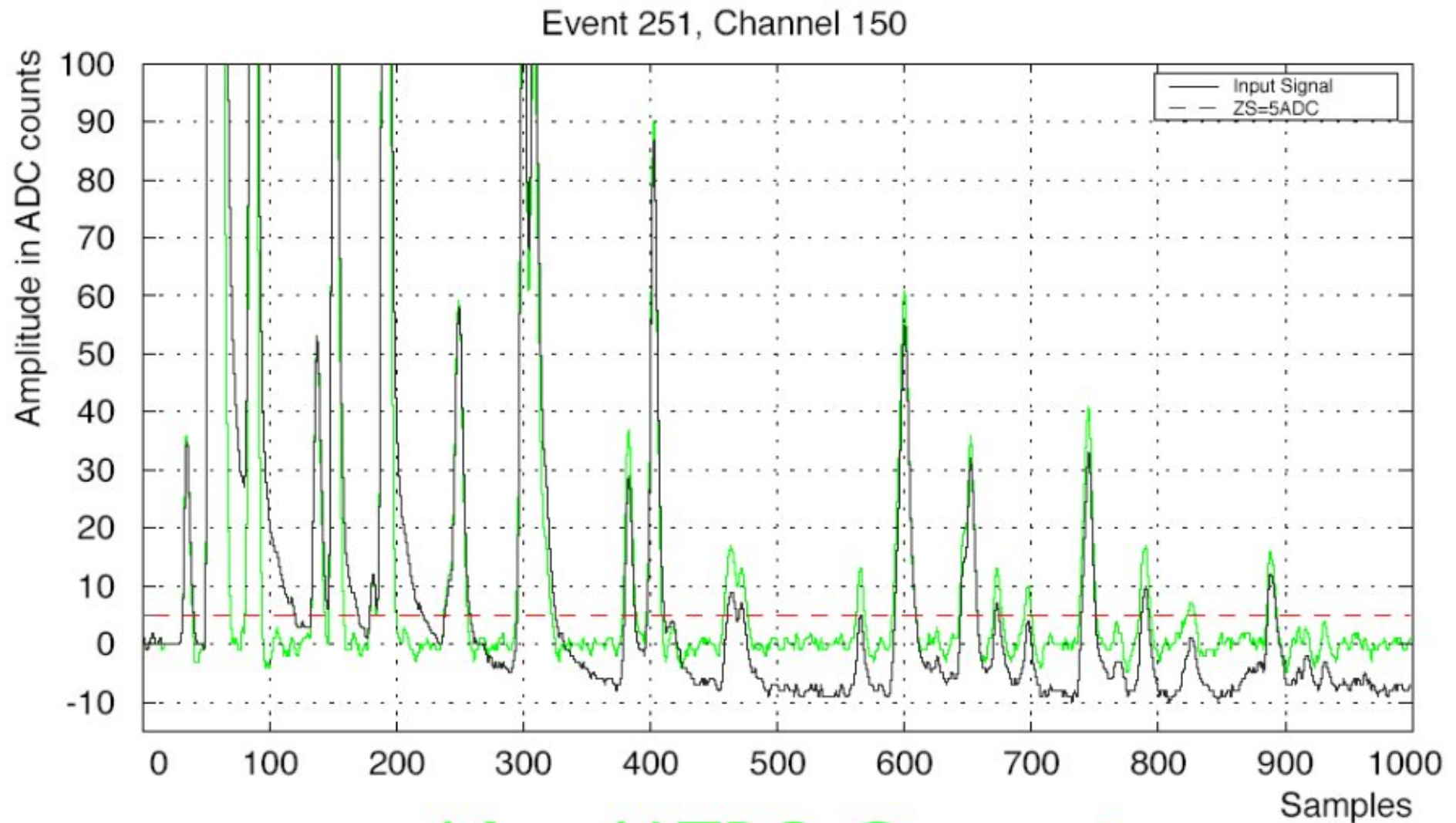


electronics needs to be clever:

- zero suppression

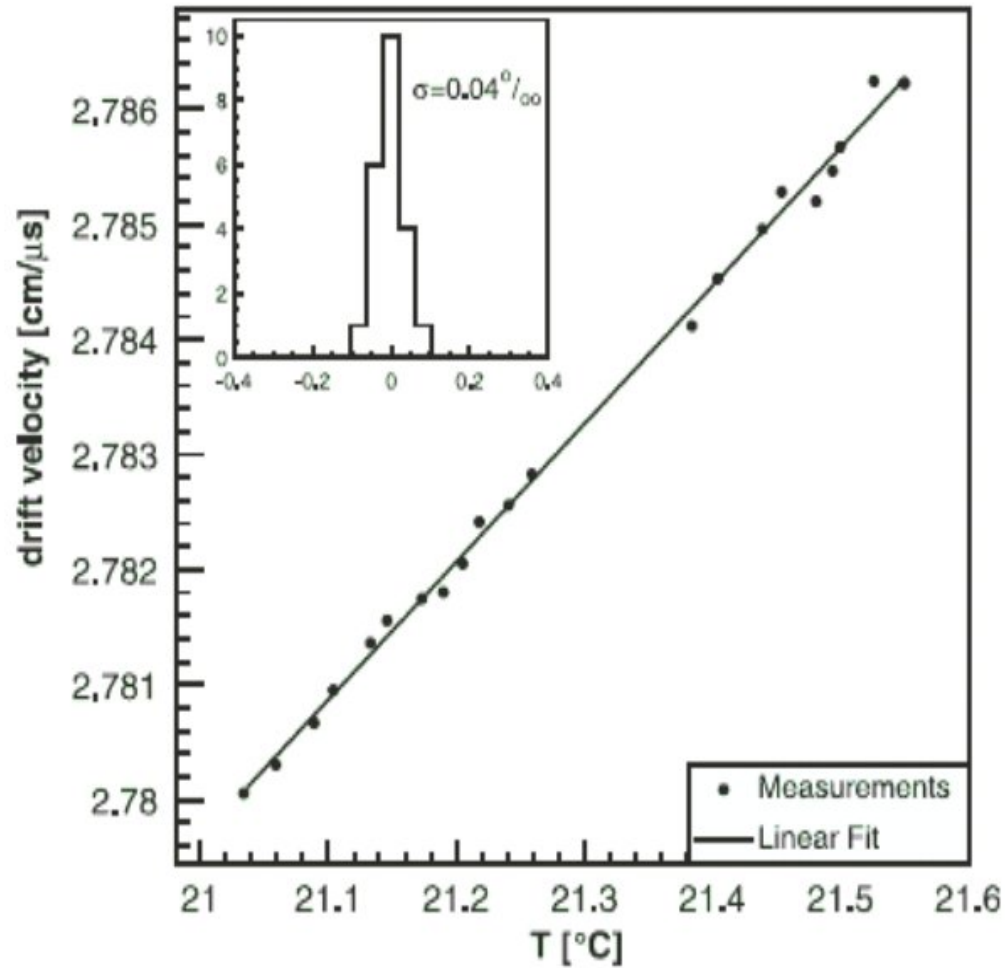
- base line restoration

- etc. → put a lot of intelligence into digital chip after ADC, the ALTRO



After ALTRO Correction

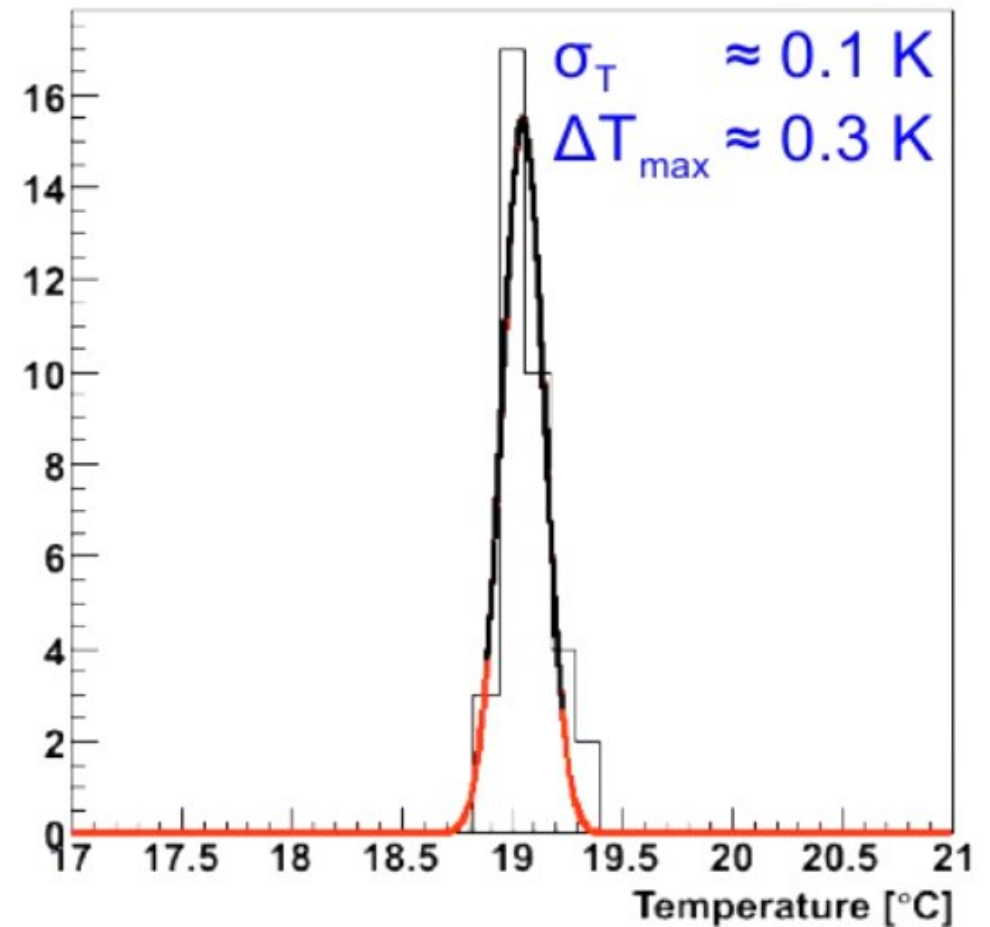
# ALICE TPC: drift velocity



converts time into z coordinate  
extreme precision needed ...  
measured with a small TPC  
(using laser for gas ionization)

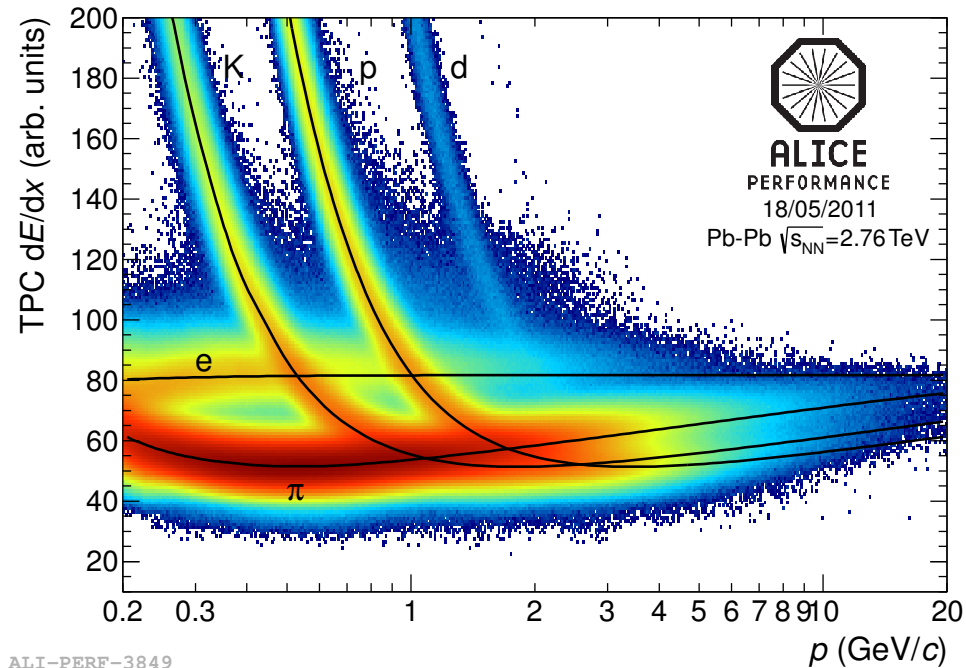
J. Wiechula et al., NIM A 548 (2005) 582

requires temperature stability of 0.1 K  
TPC FEE dissipates 27 kW  
TRD as direct neighbor 60 kW  
60 independent cooling circuits  
500 temperature sensors





# Performance of the ALICE TPC: particle identification

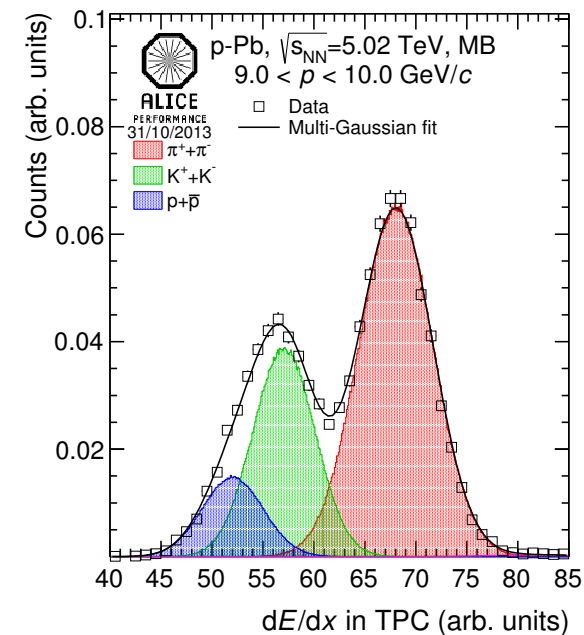
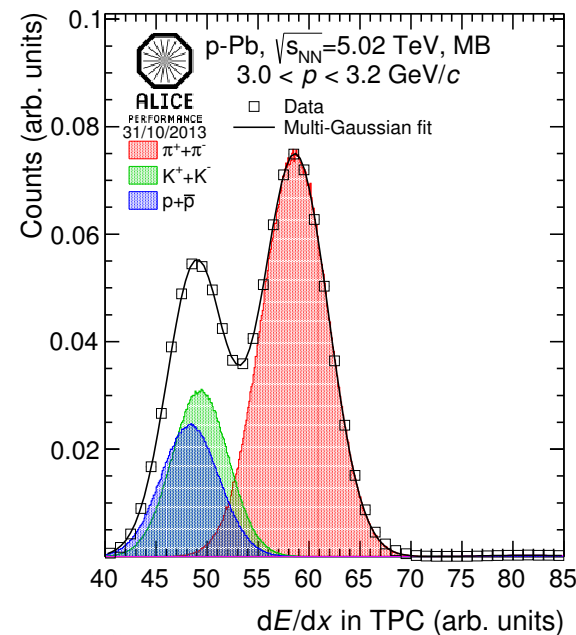
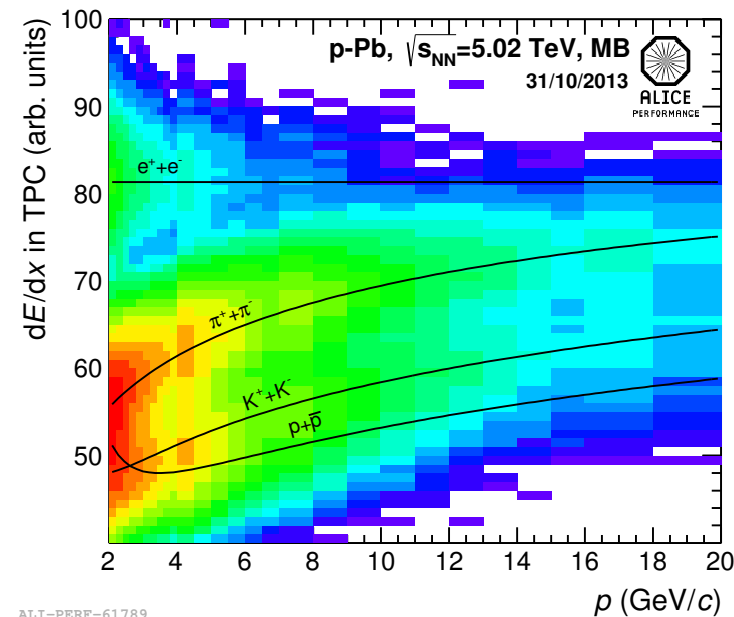


$$\frac{\sigma(dE/dx)}{dE/dx} = 5.2\% \text{ to } 6.5\%$$

(pp to central Pb-Pb)

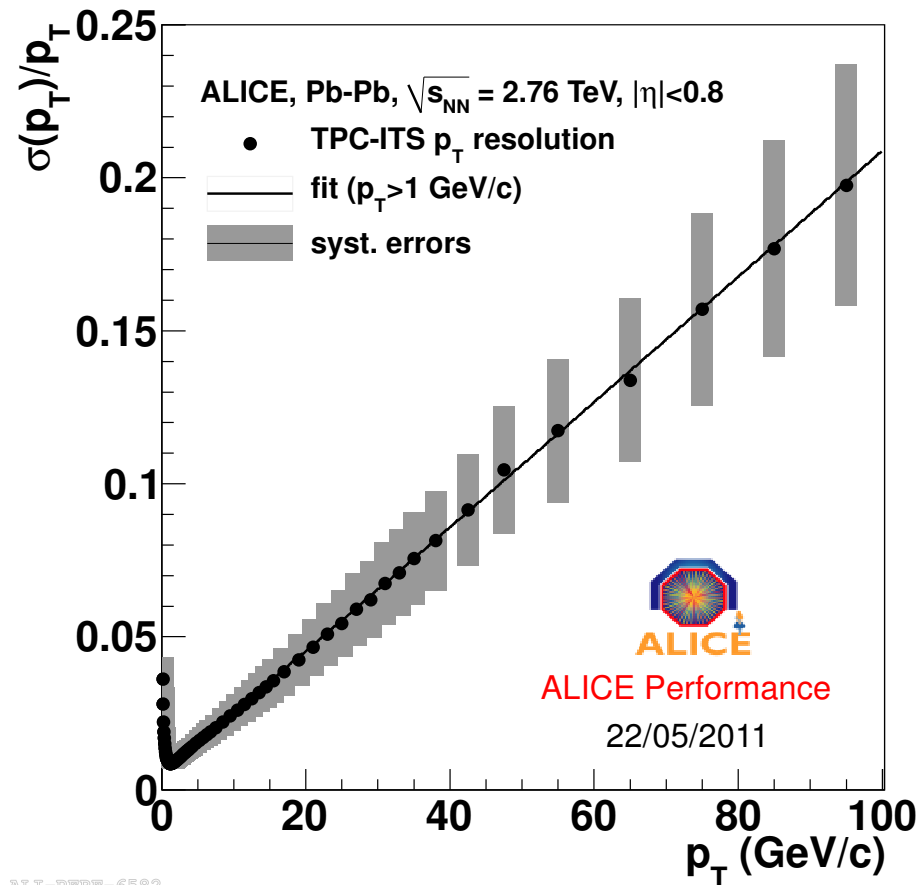
crossings: use of TOF to resolve ambiguity

statistical separation possible even in relativistic rise region





# Performance of the ALICE TPC: momentum resolution



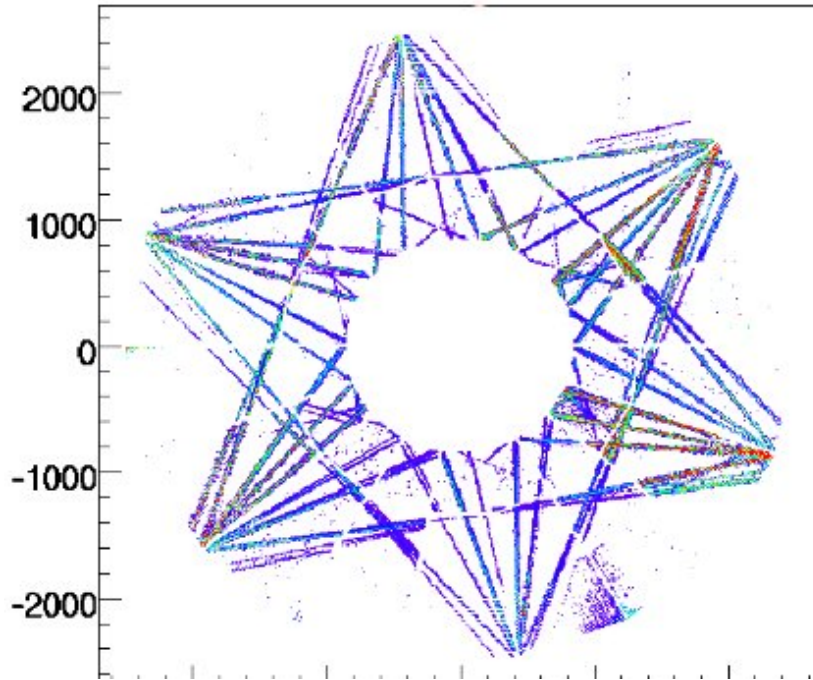
TPC standalone  $p_{\perp}$ -resolution

resolution at large  $p_{\perp}$  is improved by a factor of about 3 if vertex is included in fit

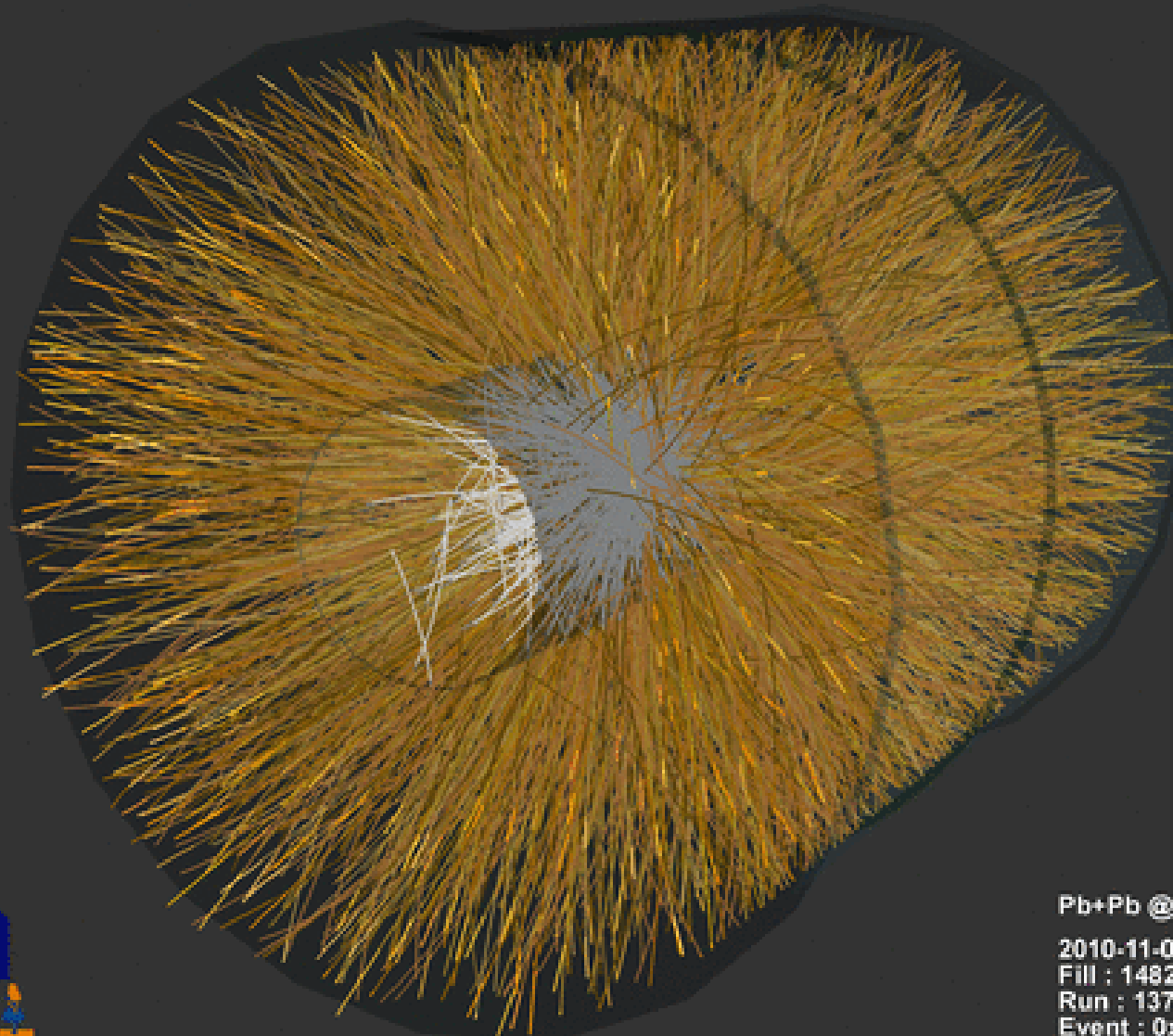
further improvement by inclusion of track segments of Inner Tracker System and Transition Radiation Detector

# TPC fully instrumented and installed in ALICE on Jan. 6, 2007

laser tracks



# ALICE TPC up and running



Pb+Pb @  $\sqrt{s} = 2.76$  ATeV

2010-11-08 11:30:46

Fill : 1482

Run : 137124

Event : 0x00000000D3BBE693